Paleoceanography and Paleoclimatology

RESEARCH ARTICLE
10.1029/2023PA004638

Key Points:

- The gametogenic crust of planktic foraminifera have lower trace elements compared to uncrusted shells collected from the same surface tow
- Stable isotope comparisons indicate that foraminifera develop crusts deeper in the water column than their average living depth habitat
- Application of culture calibrations from TE-enriched uncrusted shells to crusted fossil records may produce inaccurate paleoreconstructions

Supporting Information:

Supporting Information may be found in the online version of this article.

Correspondence to:

B. N. Hupp,
bhupp@gmu.edu

Citation:

Hupp, B. N., & Fehrenbacher, J. S. (2023). Geochemical differences between alive, uncrusted and dead, crusted shells of *Neogloboquadrina pachyderma*: Implications for paleoreconstruction. *Paleoceanography and Paleoclimatology*, *38*, e2023PA004638. https://doi.org/10.1029/2023PA004638

Received 11 MAR 2023
Accepted 25 SEP 2023

Author Contributions:

Conceptualization: Brittany N. Hupp, Jennifer S. Fehrenbacher
Data curation: Brittany N. Hupp
Formal analysis: Brittany N. Hupp
Funding acquisition: Brittany N. Hupp, Jennifer S. Fehrenbacher
Investigation: Brittany N. Hupp, Jennifer S. Fehrenbacher
Methodology: Brittany N. Hupp, Jennifer S. Fehrenbacher
Project Administration: Brittany N. Hupp, Jennifer S. Fehrenbacher
Resources: Brittany N. Hupp, Jennifer S. Fehrenbacher
Supervision: Brittany N. Hupp, Jennifer S. Fehrenbacher
Visualization: Brittany N. Hupp, Jennifer S. Fehrenbacher

Geochemical Differences Between Alive, Uncrusted and Dead, Crusted Shells of *Neogloboquadrina pachyderma*: Implications for Paleoreconstruction

Brittany N. Hupp[1,2,3] and Jennifer S. Fehrenbacher[2]

[1]NOAA Climate and Global Change Postdoctoral Fellowship Program, CPAESS, UCAR, Boulder, CO, USA, [2]College of Earth, Ocean, and Atmospheric Sciences, Oregon State University, Corvallis, OR, USA, [3]Department of Atmospheric, Oceanic and Earth Sciences, George Mason University, Fairfax, VA, USA

Abstract Planktic foraminiferal-based trace element-calcium ratios (TE/Ca) are a cornerstone in paleoceanographic reconstructions. While TE-environment calibrations are often established through culturing experiments, shell growth in culture is not always consistent with growth in a natural setting. For example, many species of planktic foraminifera thicken their shell at the end of their life cycle, producing a distinct "gametogenic" crust. Crust is common in fossil foraminifers, however, shells grown in culture do not often develop a thick crust. Here, we investigate potential vital effects associated with the crusting process by comparing the trace element (Mg/Ca, Na/Ca, Ba/Ca, Sr/Ca, Mn/Ca, Zn/Ca) and stable isotope ($\delta^{13}C$, $\delta^{18}O$) composition of alive, fully mature, uncrusted shells to recently deceased, crusted shells of *Neogloboquadrina pachyderma* collected from the same plankton tows off the Oregon (USA) coast. We find that uncrusted ($N = 55$) shells yield significantly higher Ba/Ca, Na/Ca, Mn/Ca, and Sr/Ca than crusted ($N = 66$) shells, and crust calcite records significantly lower TE/Ca values for all elements examined. Isotopic mixing models suggest that the crust calcite accounts for ~40%–70% of crusted shell volume. Comparison of foraminiferal and seawater isotopes indicate that *N. pachyderma* lives in the upper 90 m of the water column, and that crust formation occurs slightly deeper than their average living depth habitat. Results highlight the necessity to establish calibrations from crusted shells, as application of calibrations from TE-enriched uncrusted shells may yield attenuated or misleading paleoceanographic reconstructions.

Plain Language Summary The chemistry of fossil shells of planktic foraminifera, a type of marine zooplankton found throughout the global surface ocean, are commonly investigated to reconstruct past ocean and climate conditions. The chemistry of foraminiferal shells has been found to be reflective of the physical and chemical conditions of the water the shells grew within. However, biological processes can also affect shell chemistry, which may interfere with the way fossil shell chemistry is interpreted in past climate reconstructions. Here, we investigate how planktic foraminiferal shell thickening or "crusting," which occurs just after reproduction and just prior to death, could change the chemistry of a foraminiferal shell. To explore this question, the trace element and stable isotope shell chemistry was examined in populations of alive, fully mature, uncrusted specimens and recently deceased, crusted specimens collected from the same surface ocean plankton tows. Results show that crusted shells tend to record lower trace element signatures then uncrusted shells, and investigation of trace element geochemistry within the shell wall shows that this is due to crusts having lower trace element concentrations. Changes to shell chemistry associated with crusting will need to be considered when establishing quantitative relationships between planktic foraminiferal shell chemistry and environmental conditions.

1. Introduction

Evaluation of trace element geochemistry, primarily trace element/Ca (TE/Ca) ratios such as Mg/Ca, of planktic foraminifera has become a cornerstone of paleoceanographic reconstructions (Allen et al., 2016; Katz et al., 2010). Although Mg/Ca of foraminifera has been well-studied as a sea surface temperature proxy (Anand et al., 2003; Hönisch et al., 2013; Lea et al., 1999; Martínez-Botí et al., 2011; Nürnberg et al., 1996; Russell et al., 2004), advances in technology and proxy understanding have led to greater investigation and utilization of other TE/Ca ratios (e.g., Ba/Ca, Mn/Ca, Na/Ca) to evaluate past ocean-climate change (Davis et al., 2020; Fritz-Endres et al., 2022; Mezger et al., 2016; Watkins et al., 2021; Wit et al., 2013). With the development of any new proxy

Writing – original draft: Brittany N. Hupp, Jennifer S. Fehrenbacher
Writing – review & editing: Brittany N. Hupp, Jennifer S. Fehrenbacher

in biological archives, it is necessary to not only constrain the primary environmental signal driving geochemical signatures, but also identify potential interference by vital effects, the biological impacts on shell geochemistry (Niebler et al., 1999; Schiebel & Hemleben, 2017).

In general, fossil foraminiferal shells are an amalgamation of several stages of biotic, and in some cases abiotic, calcite growth (Branson et al., 2015; Hemleben et al., 1989). The biotic calcite stages include primary "ontogenetic" calcite and, in some species, secondary "gametogenic" calcite. Primary calcite is typically porous, exhibits pronounced laminations separated by organic layers, and for spinose species, acts as a base for spines to be supported (Branson et al., 2015). Many species of planktic foraminifera used in paleoreconstructions also add additional biotic calcite during or following reproduction and just prior to death, recognized as a "gametogenic crust" (Figure 1). This distinct gametogenic crust has long been identified as a feature of many planktic foraminiferal species (Bé, 1980; Bé & Lott, 1964; Caron et al., 1990). Lastly, an additional abiotic crust may be found in some fossil foraminifers that is attributed to postdepositional diagenetic processes occurring on the seafloor (Branson et al., 2015).

Advancements in in situ methodologies, such as laser-ablation inductively coupled plasma mass spectrometry (LA-ICP-MS), has allowed for greater insight into intrashell TE variability in foraminiferal shells as a means to investigate potential vital effects and relationships between different types of foraminiferal calcite (Bolton & Marr, 2013; Eggins et al., 2003; Steinhardt et al., 2015). LA-ICP-MS profiles from several different planktic foraminiferal species has shown that the gametogenic crust often yields lower TE/Ca values than the calcite grown throughout most of the foraminifers' early life in the surface ocean (i.e., the early ontogenetic, or "lamellar," calcite; Table 1). However, differences in TE/Ca between crust and early ontogenetic calcites are not found in all species nor is there a consistent crust "signature" found within a given species (e.g., *Trilobatus sacculifer*; Eggins et al., 2003). Intrashell trace element investigations have focused primarily on Mg/Ca and thus our knowledge of intrashell variability of other TE/Ca proxies is limited (Table 1).

Similar investigations have delineated differences in isotopic composition between crusted and uncrusted foraminiferal shells (Bauch et al., 2002; Blanc & Bé, 1981; Kozdon et al., 2009; Livsey et al., 2020; Mulitza et al., 1997; Schweitzer & Lohmann, 1991; Vergnaud Grazzini, 1976). In several species, $\delta^{18}O$ values of crust calcite have been found to record higher values than the ontogenetic calcite, suggesting that the addition of gametogenic crust occurs deeper in the water column relative to the foraminifers living depth habitat (Duplessy et al., 1981). These isotopic differences have fueled hypotheses, which are still under debate (Meilland et al., 2021) surrounding reproductive strategies involving depth migration during gametogenesis (Hemleben et al., 1989; Schiebel & Hemleben, 2017).

Vital effects associated with foraminiferal ontogeny, and related differences in shell geochemistry, can have prolific consequences in paleoreconstructions if not properly considered. Many calibrations used to reconstruct past ocean conditions are derived from culturing studies whereby live foraminifera are collected from the surface ocean and brought back to the lab to be grown under controlled conditions. While culturing studies strictly constrain environmental controls on biogeochemical processes, they do not always well-simulate a foraminifer's natural habitat, and thus growth in culture is not always consistent with growth in nature. For example, shells grown in culture do not always develop a thick crust, even after gametogenesis when the crust is thought to form (Davis et al., 2017; Fehrenbacher et al., 2017). However, fossil foraminiferal shells used for paleoreconstructions typically display thick gametogenic crusts. Considering known geochemical differences between the crust and ontogenetic portions of crusted shells, it is possible that applying calibrations developed in the laboratory using noncrusted shells to crusted-shell fossil specimens may result in misleading paleoceanographic reconstructions. Here, we further investigate this potential complication by comparing the trace element (Mg, Na, Ba, Sr, Mn, Zn) and stable isotope ($\delta^{13}C$, $\delta^{18}O$) composition of alive, fully mature, uncrusted (pregametogenic) shells to recently deceased, crusted shells of *Neogloboquadrina pachyderma* collected from the same discrete plankton tows. Because shells were collected from the surface ocean, the "crusted" shells mentioned henceforth refer to shells composed of primary ontogenetic calcite and gametogenic crust, and do not include additional secondary diagenetic crust. Intrashell trace element variability is also examined in order to characterize geochemical differences between the crusted and ontogenetic portions of the shell wall. Lastly, stable isotope compositions of alive, uncrusted and dead, crusted populations are compared to stable isotope profiles of the water column measured from the same plankton tow collection sites to make inferences about where crusting occurs in the water column. By evaluating a species critical to paleoreconstructions at high latitudes, we aim to characterize the extent of geochemical differences between crusted and uncrusted shells, expand the analytes of interest beyond Mg/Ca (the focus of most studies—see Table 1), and explore the implications of such differences for paleoreconstruction.

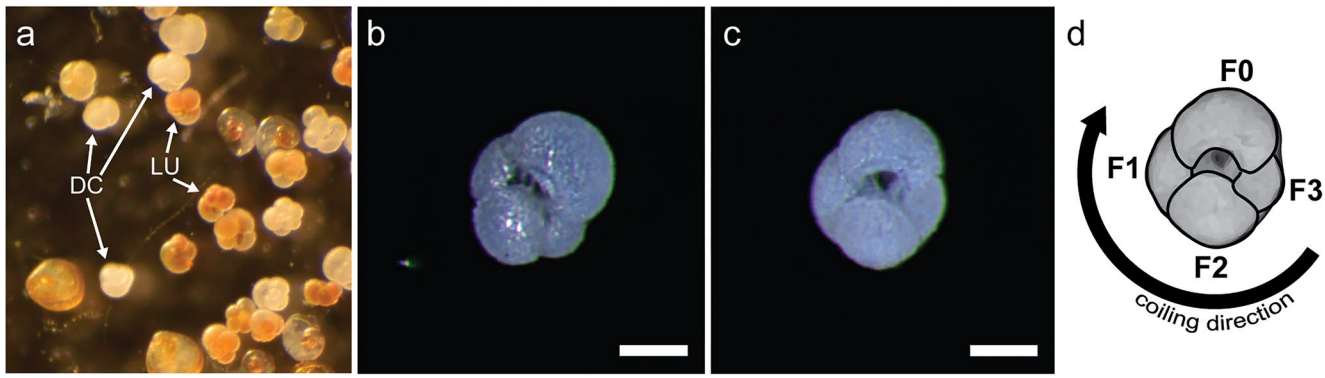

Figure 1. Representative examples of (a) a mixture of live, uncrusted (LU) and dead, crusted (DC) shells in a plankton tow sample, (b) a live-caught uncrusted *Neogloboquadrina pachyderma* shell that has been cleaned to remove the colorful cytoplasm, and (c) a cleaned, dead, crusted shell of *N. pachyderma*. Scale bars are equal to 100 µm. (d) A schematic illustrating the relative position of the outer whorl chambers examined in this study.

2. Materials and Methods

2.1. Sampling

Neogloboquadrina pachyderma were collected from two stations along the Newport Hydrographic (NH) Line off the Oregon coast: NH85 (44.652°N, 126.050°W) and NH45 (44.652°N, 125.117°W) in May 2022 (Figure 2). *N. pachyderma* are an asymbiotic, nonspinose taxon found abundantly in the study region when cooler waters are present (Lane et al., 2023; Ortiz & Mix, 1992; Takagi et al., 2019), and they serve as an important species to reconstruct polar to subpolar paleoceanographic conditions. A 150 µm plankton tow net was used to sample the uppermost 200 m of the water column, sampled as two continuous tows from 200 m depth to the surface. While *N. pachyderma* have been found at greater depth habitats in other regions (i.e., Greco et al., 2019), the sampling was constrained to the upper 200 m of the water column to ensure that we were sampling populations calcifying from the same

Table 1
Summary of TE/Ca Differences Observed Between the Crust and Ontogenetic Calcites as Found in the Published Literature

Species	Mg/Ca	Na/Ca	Sr/Ca	Ba/Ca	Mn/Ca	Zn/Ca
Neogloboquadrina pachyderma	Lower[1,3], ND[2]	Lower[2]	Lower[2]	Lower[2]	Lower[2]	Lower[2]
N. incompta	Lower[3,4,5]	–	ND[2]	–	–	–
N. pachyderma-dutertrei (P-D) intergrade	Lower[5]	–	ND[5]	–	–	–
N. dutertrei	Lower[1,4,6,7,8]	–	ND[1,6]	Lower[1]	Lower[1,6,7]	Lower[1]
Globorotalia truncatulinoides	Lower[4,9]	–	–	–	–	–
G. inflata	Lower[5,10]	–	ND[5,10]	Lower[10]	Lower[10]	–
G. scitula	Lower[8,10]	–	ND[10]	Lower[10]	Lower[10]	–
G. tumida	Lower[11,12]	–	ND[12]	–	–	–
G. menardii	Lower[4]	–	–	–	–	–
Globogerina bulloides	Lower[13]	–	–	–	–	–
Trilobatus sacculifer	Higher[14]; Lower[1,15], ND[1,11]	Higher[16]	ND[1]	Lower[1]	Lower[1]	Lower[1]
Globigerinoides ruber	ND[1,4]	–	ND[1]	ND[1]	ND[1]	ND[1]
G. conglobatus	Lower[4]	–	–	–	–	–
Pulleniatina obliguiloculata[a]	Lower[8]	–	–	–	–	–
Orbulina universa	Lower[4]	–	–	–	–	–

Note. TE/Ca comparisons are labeled as the crust calcite either being found to be lower, higher, or no difference (ND) in TE/Ca values when compared to the ontogenetic calcite of the same shell. References are as follows: [1]Eggins et al. (2003); [2]this study; [3]Davis et al. (2017); [4]Sadekov et al. (2005); [5]Bolton and Marr (2013); [6]Pena et al. (2008); [7]Jonkers et al. (2012); [8]Steinhardt et al. (2015); [9]Duckworth (1977); [10]Hathorne et al. (2009); [11]Brown and Elderfield (1996); [12]Branson et al. (2015); [13]Elderfield and Ganssen (2000); [14]Nürnberg et al. (1996); [15]Rosenthal et al. (2000); and [16]Bertlich et al. (2018).

[a]This comparison was not between the gametogenic crust and early ontogenetic calcite, but rather between the cortex and early ontogenetic calcite.

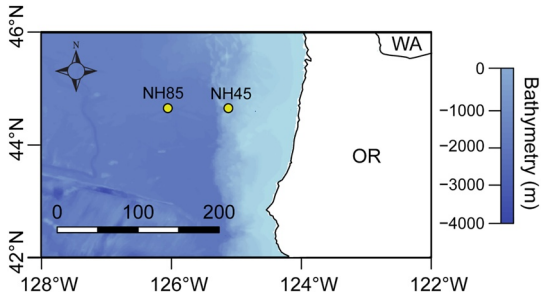

Figure 2. Bathymetric map showing the location of the two collection sites (NH85, NH45) off the Oregon coast. Distance scale bar is in kilometers (km).

water depth and that geochemical differences between alive, uncrusted and dead, crusted could be directly attributed to the process of gametogenic crust development as opposed to any additional geochemical changes associated with the shells sinking through the water column (e.g., scavenging). Previous depth-stratified tows conducted in the study region (Ortiz et al., 1996) have found minor concentrations (<0.25 individuals/m^3) of *N. pachyderma* below 200 m water depth. Fully mature, live specimens and recently deceased, crusted specimens of *N. pachyderma* were immediately wet picked from each tow, rinsed with distilled water, and placed in micropaleontological slides. Alive specimens were identified by their distinctive brightly colored cytoplasm and relatively thin shell walls, whereas the shells of recently deceased foraminifers were free of cytoplasm, appeared white under reflective light, and exhibited a thick crust (Figure 1). A total of 66 dead shells (NH85: $N = 52$; NH45: $N = 14$) and 55 alive shells (NH85: $N = 44$; NH45: $N = 11$) were collected.

Conductivity-temperature-depth (CTD) profilers were used to characterize the water column at each site and showed consistent conditions at NH85 and NH45 (Figure 3), supporting the pooling together of samples from both sites. Seawater samples were collected from both study sites from the following depths: 5, 25, 50, 100, 150, 250, and 500 m, to establish stable isotope profiles. Seawater samples collected for $\delta^{13}C$ analysis of the dissolved inorganic carbon were poisoned with mercuric chloride ($HgCl_2$) immediately upon collection. Seawater samples obtained for $\delta^{18}O$ analysis were collected in scintillation vials and capped with a positive meniscus at the top of each vial to avoid atmospheric exchange post-collection.

2.2. LA-ICP-MS TE/Ca Analysis

2.2.1. Sample Preparation

Prior to geochemical analyses, specimens were rinsed and oxidatively cleaned to remove remnant organic matter, following previously established protocols, adapted for single shells (Martin & Lea, 2002). To remove any detritus, the shells were rinsed with ultrapure (milliQ) water, followed by methanol, and then given an additional rinse with ultrapure water. Next, shells were submerged in a 1:1 solution of 30% H_2O_2 buffered with 0.1 M NaOH, and vials were placed in a hot (65°C) water bath for 10 min. The solution was removed from the sample vials, and shells were rinsed three times in ultrapure water. Shells were subsequently mounted on a slide covered with strips of carbon tape in preparation for in situ trace element analysis.

2.2.2. LA-ICP-MS Analytical Methods

All specimens were analyzed via LA-ICP-MS to evaluate trace element geochemistry. Shells were analyzed using a Thermo Scientific iCAP RQ inductively coupled plasma mass spectrometer coupled to an Applied Spectra RESOlution laser ablation system in the Keck Collaboratory for Plasma Spectrometry at Oregon State University. Ten

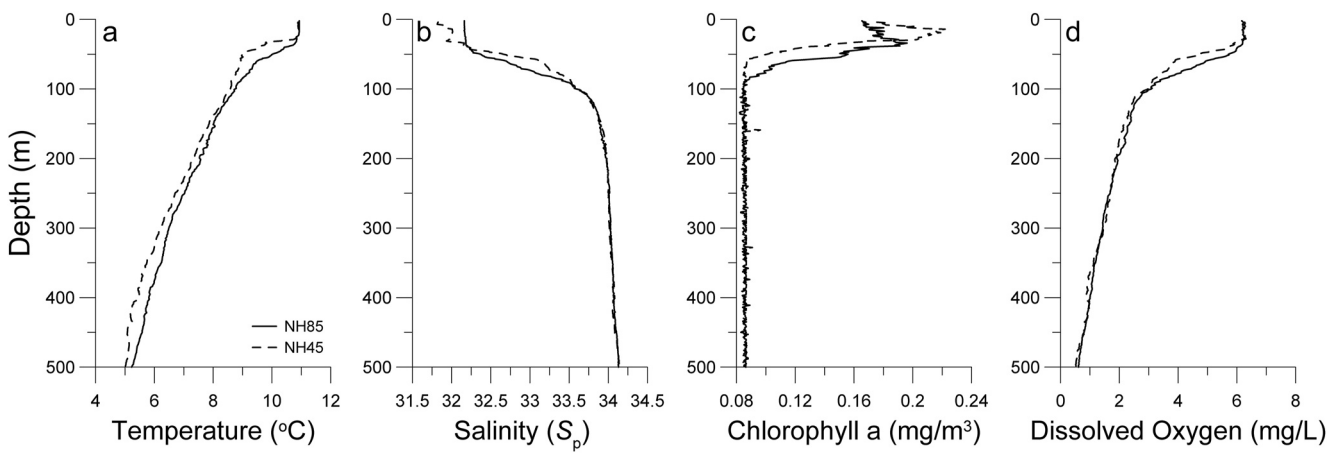

Figure 3. Profiles of the uppermost 500 m of the water column from NH85 (solid line) and NH45 (dashed line) showing the (a) temperature, (b) salinity, (c) chlorophyll content, and (d) dissolved oxygen measured from CTD casts on the day of plankton tow collections.

isotopes were measured with the following seven isotopes evaluated herein: ^{23}Na, ^{24} Mg, ^{43}Ca, ^{55}Mn, ^{66}Zn, ^{88}Sr, and ^{138}Ba. Isotopes were measured using a rapid peak-hopping procedure with the following dwell times for each isotope: ^{23}Na = 0.04 s, ^{24} Mg = 0.02 s, ^{43}Ca = 0.01 s, ^{55}Mn = 0.05 s, ^{66}Zn = 0.05 s, ^{88}Sr = 0.02 s, and ^{138}Ba = 0.05 s. Shells were ablated from the outer shell surface through to the interior of the shell at a repetition rate of 5 Hz and a laser energy of 4.0 mJ attenuated by 75%–87.5%, focused upon 24–38 μm spot sizes. The last four chambers in the final whorl, F0 (ultimate chamber) to F3 (Figure 1d), were analyzed with repeated analysis on at least one chamber per specimen to assess reproducibility (Table S1 in Supporting Information S1). Shell averages reported herein were calculated by first averaging repeated analyses on single chambers, followed by equal-weight averaging of the chamber averages. In <6% of the specimens, the F3 chamber was too small or not accessible due to the orientation of the specimen on the tape, and thus was not analyzed or included in the calculation of the whole-shell value. Analysis of shells was periodically bracketed by analysis of three standard reference materials (SRM): NIST glasses 610 and 612, and the USGS standard MACS-3. Each standard was ablated for 60 s at an energy of 5.00 mJ using a 50 μm spot size. All element concentrations were determined using NIST 610 and NIST 612, however due to consistent Na concentrations found in NIST glasses, Na was evaluated using the NIST 610 and MACS-3 SRMs. Elemental calibrations of SRMs measured throughout the analysis session yielded $r^2 \geq 0.99$.

2.2.3. Data Analysis Methods

LA-ICP-MS data were processed using the Python package LA-Tools (Branson et al., 2019) which follows established data reduction protocols (Longerich et al., 1996). Data processing protocols include despiking and signal smoothing to remove outliers, evaluating and applying any necessary drift correction using the bracketing SRM analyses, and removing average background counts from each data point. The mean TE/Ca for each profile (i.e., individual chamber analysis) is then calculated by normalizing to the known trace element concentrations of the drift-corrected SRM standards (Jochum et al., 2011).

Several approaches were employed to investigate differences between whole-shell, intrashell, and chamber-to-chamber variability. The distributions of whole-shell and individual chamber (i.e., F0, F1, F2, F3; Figure 1d) TE/Ca values were compared between the uncrusted (alive upon collection) and crusted (dead) shells. A Shapiro-Wilks test determined that nearly every population was nonnormally distributed, and thus a Mann-Whitney test was used to evaluate if the uncrusted versus crusted trace element chemistries were statistically significantly different (denoted by a red star in Figure 4).

The intrashell depth profiles are used to explore intrashell TE variability and reflect changes in trace element geochemistry as the laser ablated from the outside of the shell through the shell wall (e.g., Figure 5). To aid in the interpretation of the intrashell geochemical variability on a population scale, the TE/Ca data from the depth profiles were plotted on a 1:1 plot, where the average of the outer 50% of the data from each individual depth profile (reflecting mostly crust calcite, if present) was plotted against the inner 50% average of data obtained from the same specimen (reflective of the ontogenetic calcite) (Figures S1 and S2 in Supporting Information S1). The difference in TE/Ca between the inner 50% and outer 50% of each depth profile (ΔTE/Ca$_{\text{inner-outer}}$) was calculated and plotted relative to a zero line (Figure 6). If the inner, ontogenetic calcite is more enriched in a given TE, the difference will plot above the zero line in Figure 6 (above the 1:1 line in Figures S1 and S2 in Supporting Information S1). If the outer, crust calcite yields higher TE concentrations, the inner-outer difference will plot below the zero line in Figure 6 (below the 1:1 line in Figures S1 and S2 in Supporting Information S1). If there are no distinct differences in the concentration of a given TE between the inner and outer calcites, values will plot near or on the zero line in Figure 6 (on or near the 1:1 line in Figures S1 and S2 in Supporting Information S1). The distributions for whole-shell values for the alive, uncrusted shells are compared to the distributions of the inner 50% spectral averages and outer 50% spectral averages of the dead crusted shells (Figure 7). Inner 50% chamber spectral averages, outer 50% chamber spectral averages, TE/Ca shell averages, and full TE/Ca spectra can be found in Hupp and Fehrenbacher (2023).

2.3. Stable Isotope (δ^{13}C and δ^{18}O) Analysis

2.3.1. Stable Isotope (δ^{13}C and δ^{18}O) Analysis of Foraminiferal Shells

Study specimens were analyzed for stable carbon (δ^{13}C) and oxygen (δ^{18}O) isotopes following completion of LA-ICP-MS analysis. Stable isotope measurements were performed at the Oregon State University Stable Isotope Laboratory using a Thermo Scientific Kiel IV carbonate device interfaced to a Thermo Scientific MAT 253 dual-inlet gas-source isotope ratio mass spectrometer. Two to three foraminiferal shells of the same life stage (dead versus live) were pooled together for each individual stable isotope analysis due to low masses. In total,

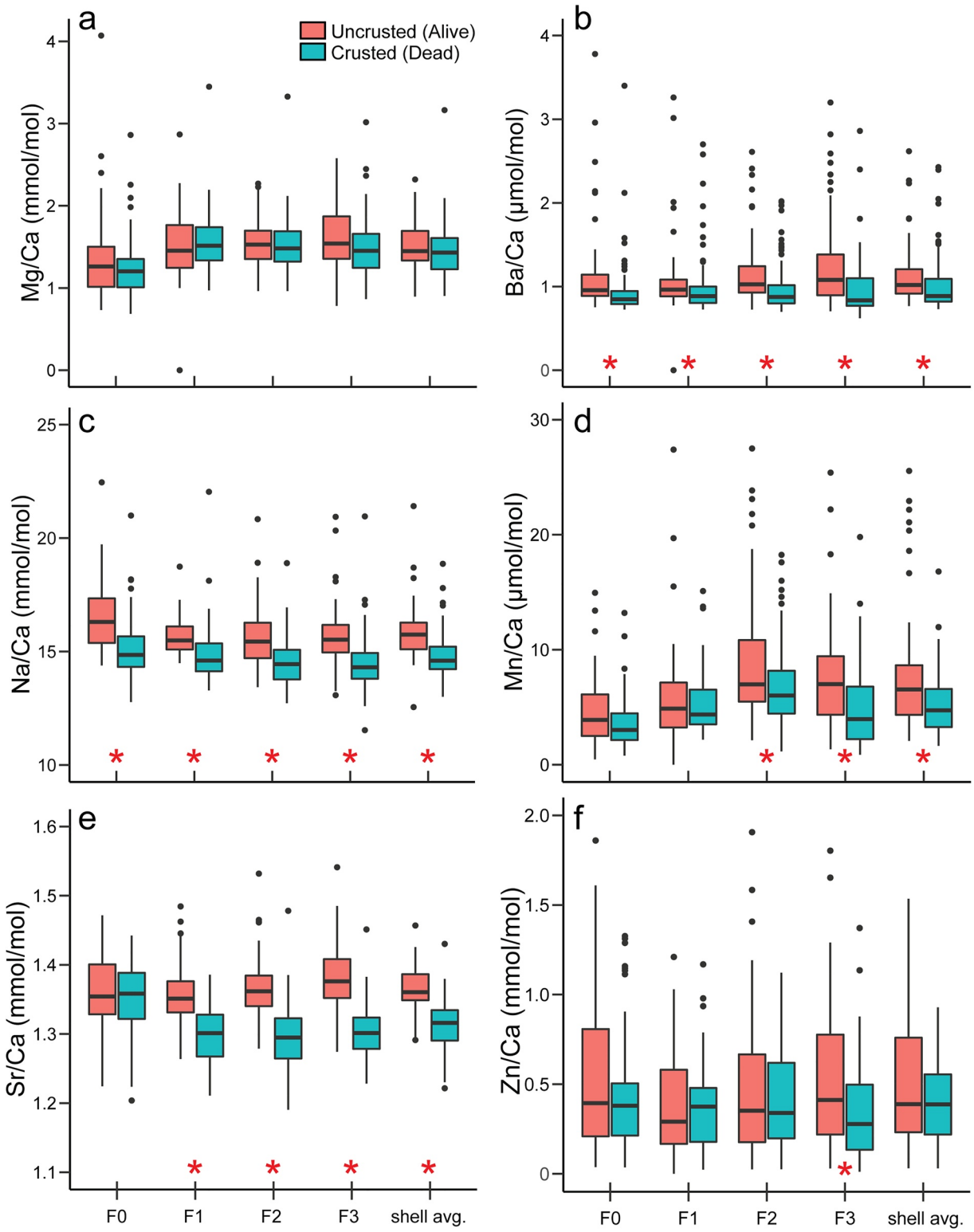

Figure 4. Boxplots showing the distributions of *N. pachyderma* TE/Ca data from each individual chamber in the final whorl (F0, F1, F2, F3) and the whole-shell average for the alive-caught, uncrusted shells (pink) and dead, crusted shells (blue). (a) Mg/Ca, (b) Ba/Ca, (c) Na/Ca, (d) Mn/Ca, (e) Sr/Ca, and (f) Zn/Ca. Red stars denote significant differences between the crusted and uncrusted populations (Mann-Whitney test, p-value < 0.05).

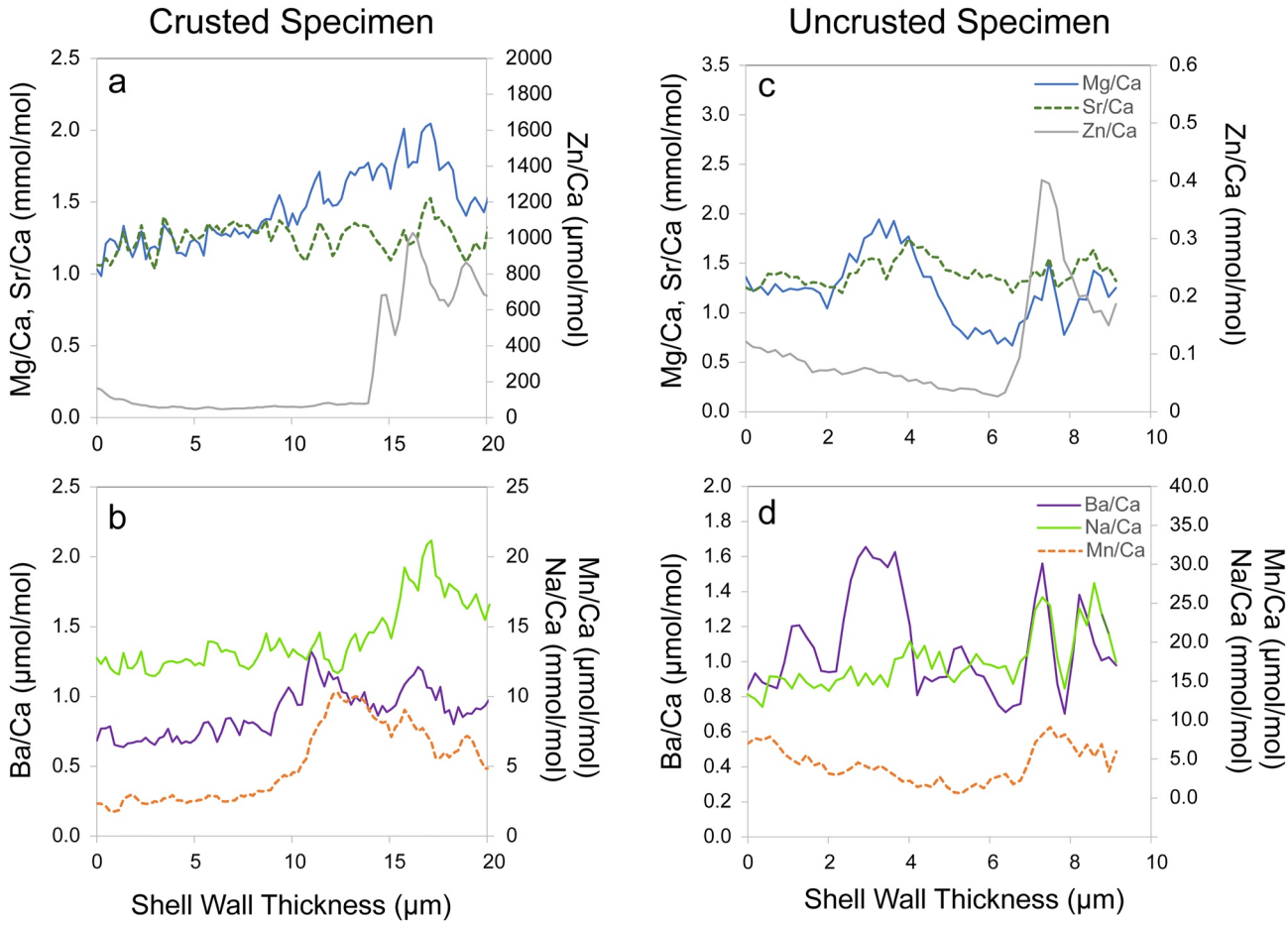

Figure 5. Example TE/Ca depth profile for (a and b) a crusted specimen (Shell #100, F2 chamber) and (c and d) an uncrusted specimen (Shell #4, F2 chamber).

23 separate analyses of dead foraminifera and 19 separate analyses of shells of alive specimens were conducted. Replicate analyses of NBS19 ($\delta^{13}C$ = 1.95‰ VPDB, $\delta^{18}O$ = −2.2‰ VPDB) and in-house standard $CaCO_3$ standard "Wiley" ($\delta^{13}C$ = −0.41‰ VPDB, $\delta^{18}O$ = −7.20‰ VPDB) resulted in an analytical precision (1SD) of ≤0.05‰ and ≤0.08‰ for $\delta^{13}C$ and $\delta^{18}O$, respectively. All shell stable isotope data can be found in Hupp and Fehrenbacher (2023).

2.3.2. Stable Isotope Analysis of Dissolved Inorganic Carbon ($\delta^{13}C_{DIC}$) and Seawater ($\delta^{18}O_{sw}$)

Seawater samples were collected from the two study sites for comparison between the isotope signatures recorded by the shells and isotope profiles of the water column (Figures 8 and 9). Seawater samples were analyzed in the Stable Isotope Laboratory at Oregon State University. The carbon isotope analysis of the dissolved organic carbon of seawater ($\delta^{13}C_{DIC}$) was analyzed using a Thermo Scientific Delta V isotope ratio mass spectrometer fitted to a gas bench. For each sample 1 mL of seawater was injected into a sealed, helium-flushed vial. Prior to analysis, 100 μL of 85% H_3PO_4 were injected into the sample vial and left to equilibrate for 8 hr. Two standards were analyzed over the course of each run to check stability and calibrate reference gases: an in-house Wiley standard and 0.7 mL of 3 mM $NaHCO_3$. Repeated analysis of standards resulted in an analytical error (standard deviation) for $\delta^{13}C$ of ±0.03‰. All $\delta^{13}C_{DIC}$ data are reported relative to VPDB (Figure 8 and Table 2).

Oxygen isotope analysis of seawater ($\delta^{18}O_{sw}$) samples were conducted using a Thermo Scientific Delta PlusXL mass spectrometer with a water equilibration system. Seawater samples were calibrated using three internal standards ("LROSS-6," $\delta^{18}O$ = −10.97‰; "HOT-4," $\delta^{18}O$ = −0.17‰; "Seawater," $\delta^{18}O$ = −0.55‰) scattered throughout and bracketing each run. The isotopic compositions of LROSS-6 and HOT-4 internal standards have been calibrated using the international standards VSMOW, GISP, and SLAP. Samples were analyzed using the CO_2 equilibration method and dual-inlet isotope ratio mass spectrometry, with an analytical error (standard

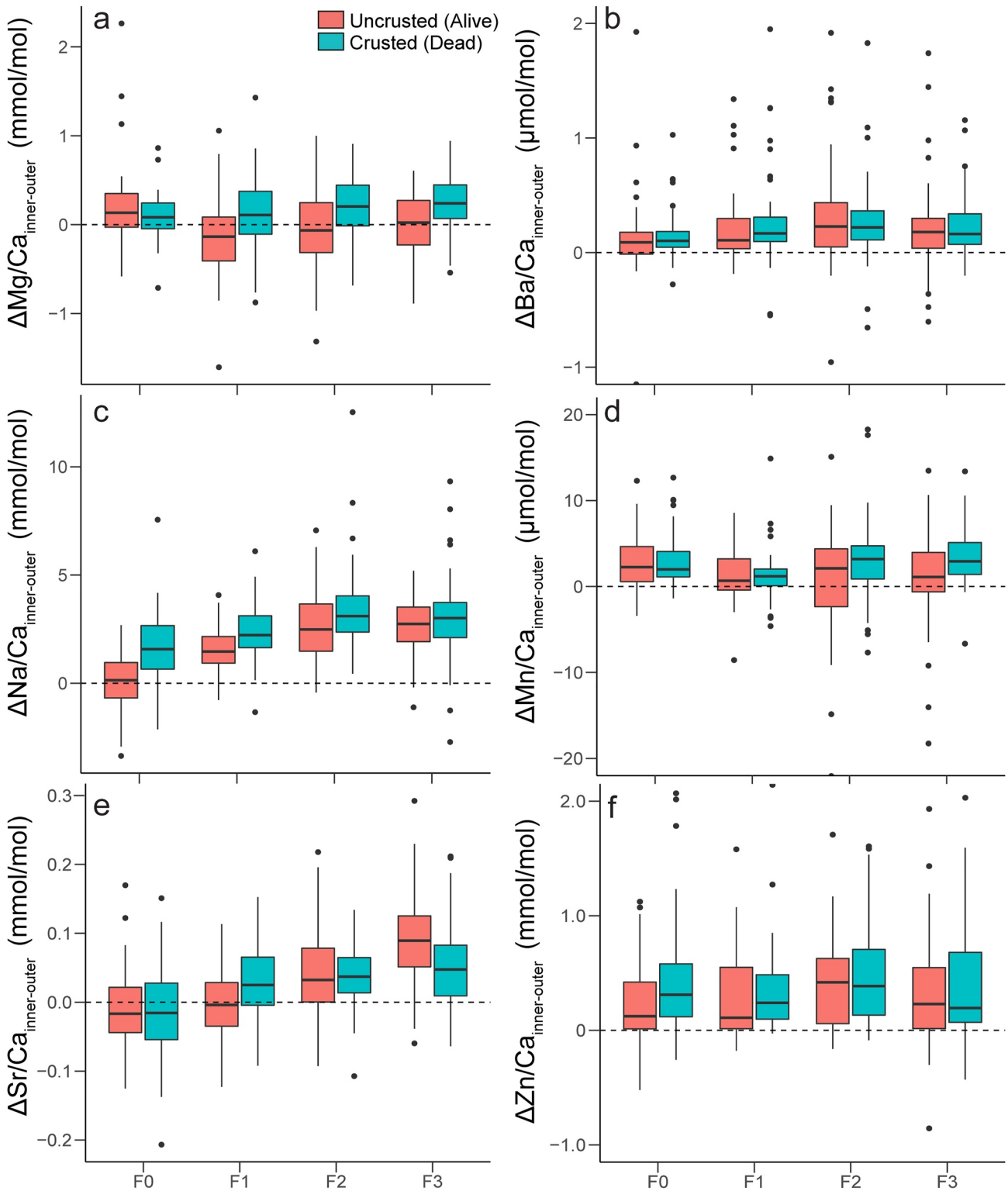

Figure 6. Boxplots showing the $\Delta TE/Ca_{inner\text{-}outer}$ distributions, where $\Delta TE/Ca_{inner\text{-}outer}$ values are calculated as the difference between the average inner 50% of a TE/Ca spectrum minus the average of the outer 50% of the same TE/Ca spectrum for each chamber of a given shell. (a) Mg/Ca, (b) Ba/Ca, (c) Na/Ca, (d) Mn/Ca, (e) Sr/Ca, and (f) Zn/Ca. Distributions derived from uncrusted shells are shown in pink whereas distributions of crusted shells are shown in blue.

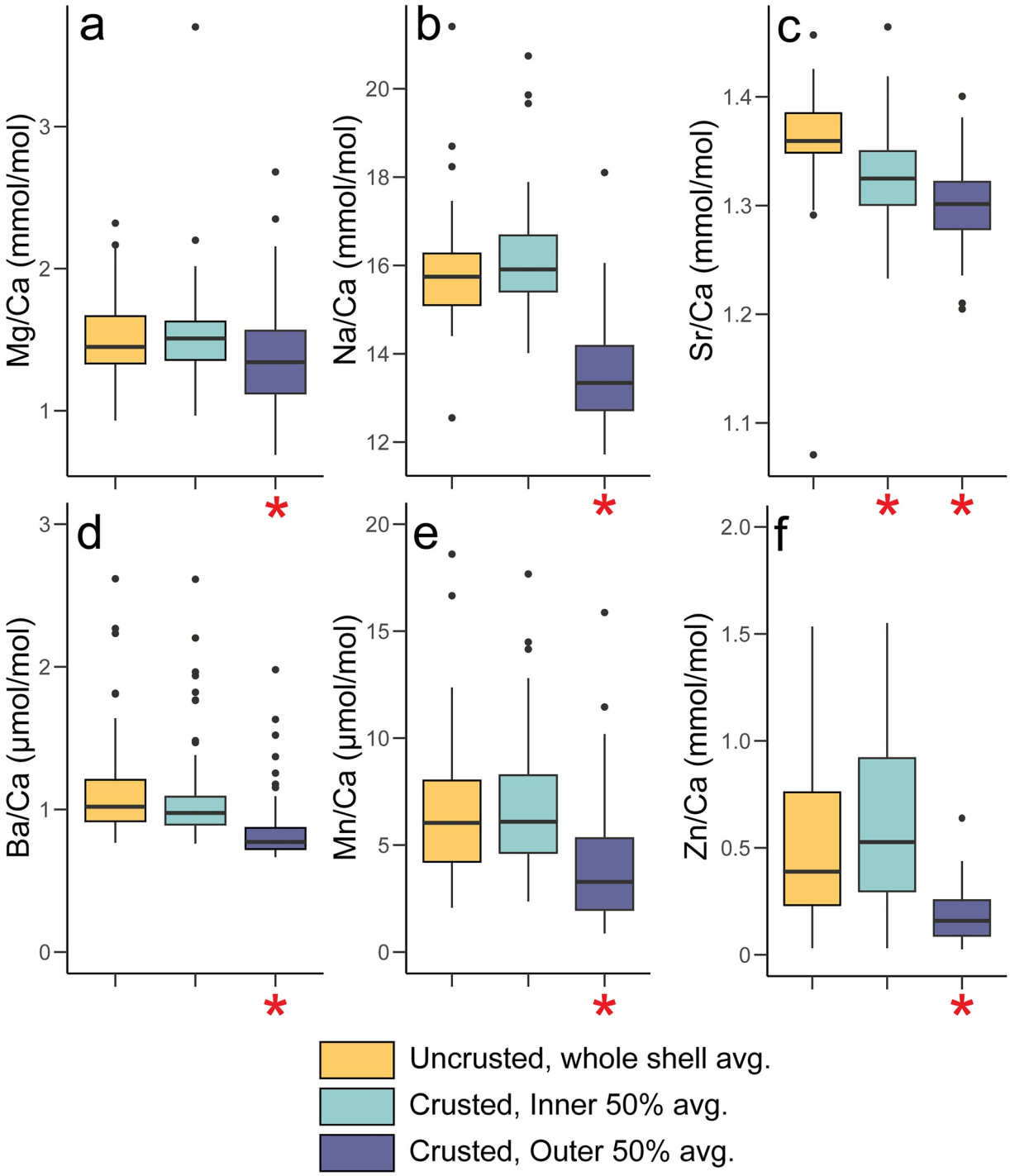

Figure 7. Boxplots of whole-shell average (a) Mg/Ca, (b) Na/Ca, (c) Sr/Ca, (d) Ba/Ca, (e) Mn/Ca, and (f) Zn/Ca values of uncrusted shells (yellow) to the inner 50% average (blue) and outer 50% average (purple) of the crusted shells. Significant differences were denoted with a red star (Mann-Whitney test, p-value < 0.05).

deviation of repeated standard runs) of ±0.05‰. All $\delta^{18}O_{sw}$ data are reported relative to VSMOW in Table 2. The predicted $\delta^{18}O$ for calcite precipitated at equilibrium from seawater ($\delta^{18}O_{calcite}$) was calculated for comparison to the $\delta^{18}O$ values of the foraminiferal shells. The predicted $\delta^{18}O_{calcite}$ value for each water depth (Table 2) was calculated using the seawater temperature (from the CTD cast), the measured $\delta^{18}O_{sw}$ values, and the following precipitation equilibrium equation from Kim and O'Neil (1997):

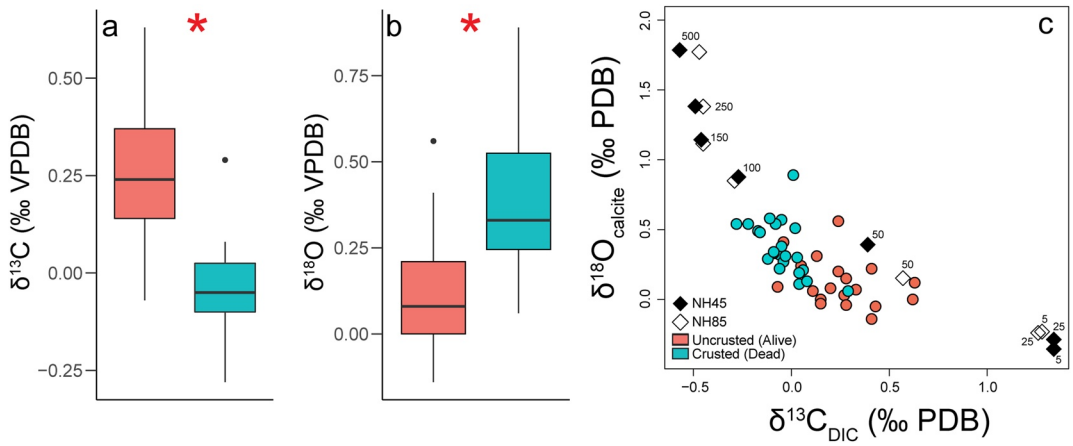

Figure 8. Boxplots of stable (a) carbon ($\delta^{13}C$) and (b) oxygen ($\delta^{18}O$) isotope values for the uncrusted (pink) and crusted (blue) shells. The uncrusted and crusted populations were found to be significantly different (Student's *t*-test) in both their carbon and oxygen isotopic compositions, as denoted by the red stars. (c) A cross plot of the carbon and oxygen isotope values for uncrusted shells (pink circles) and crusted shells (blue circles), and the $\delta^{13}C_{DIC}$ and $\delta^{18}O_{calcite}$ measured or calculated, respectively, from the water samples collected from NH45 (black diamonds) and NH85 (white diamonds). The numbers labeling each diamond denote the depth (m) at which the water sample was collected. The $\delta^{18}O_{calcite}$ values in panel (c) are the predicted $\delta^{18}O$ of calcite precipitated under equilibrium at each water depth as determined from measured $\delta^{18}O_{sw}$ and temperature, using the Kim and O'Neil (1997) equation. Note that each shell data point represents an analysis of two to three shells of the same life stage (dead versus live) from the same plankton tow that were pooled together.

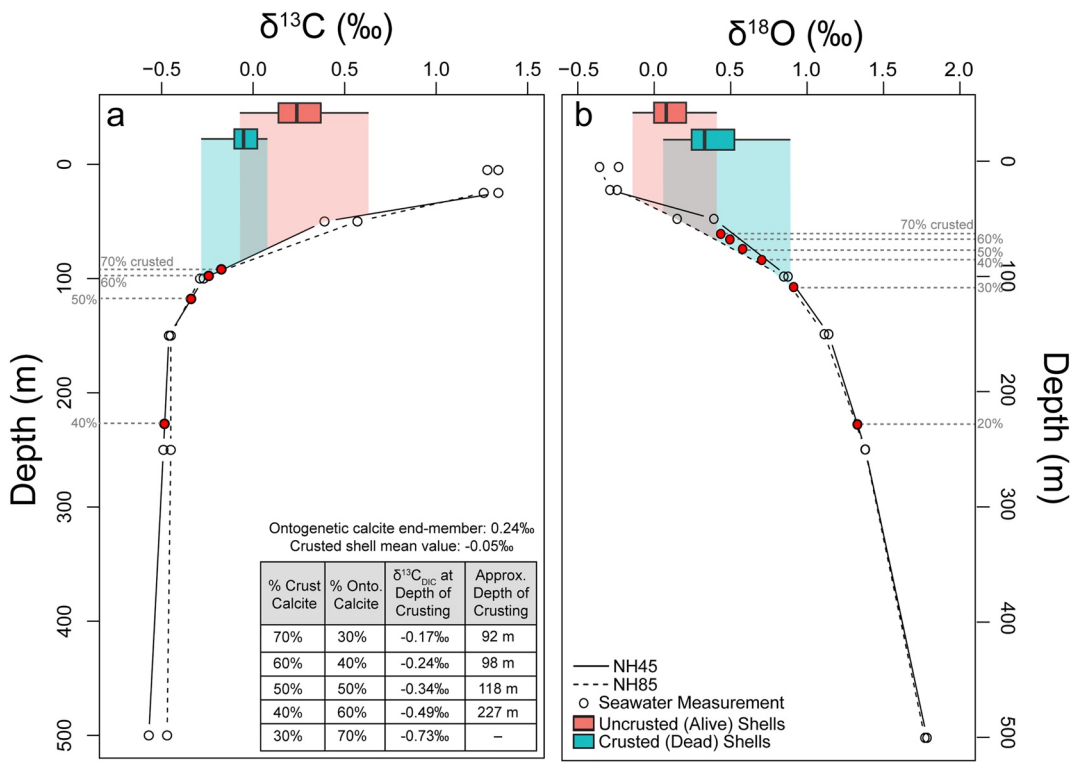

Figure 9. Comparison of (a) carbon and (b) oxygen isotope data of crusted (blue boxplots) and uncrusted (pink boxplots) shells to the $\delta^{13}C_{DIC}$ and $\delta^{18}O_{calcite}$ profiles. The $\delta^{18}O$ equilibrium calcite profile was calculated using the equation from Kim and O'Neil (1997). Red dots and associated labels demarcate the depth of crusting assuming various mixing scenarios of crust and ontogenetic calcite (Section 4.2). Mixing scenarios and estimated depths of crusting using the $\delta^{13}C$ data are included as an inlayed table in panel (a).

Table 2
Carbon ($\delta^{13}C_{DIC}$) and Oxygen ($\delta^{18}O_{sw}$) Isotope Values Measured From the Seawater Samples Collected From Each Site

Site	Latitude (°N)	Longitude (°W)	Depth sampled (m)	$\delta^{13}C_{DIC}$ (‰ VPDB)	$\delta^{18}O_{sw}$ (‰ VSMOW)	Temperature (°C)	Calculated equilibrium calcite $\delta^{18}O_{calcite}$ (‰ VPDB)
NH45	44.6517	125.117	5	1.34	−0.98	10.88	−0.36
			25	1.34	−0.92	10.83	−0.29
			50	0.39	−0.64	9.04	0.39
			100	−0.27	−0.26	8.58	0.88
			150	−0.46	−0.16	7.86	1.14
			250	−0.49	−0.19	6.70	1.38
			500	−0.57	−0.18	5.01	1.78
NH85	44.6517	126.050	5	1.28	−0.84	10.93	−0.23
			25	1.26	−0.87	10.85	−0.24
			50	0.57	−0.66	10.02	0.15
			100	−0.29	−0.25	8.75	0.85
			150	−0.45	−0.15	8.01	1.11
			250	−0.45	−0.11	7.03	1.38
			500	−0.47	−0.14	5.23	1.77

Note. Temperatures measured from the CTD and predicted $\delta^{18}O$ values for equilibrium calcite ($\delta^{18}O_{calcite}$) using the equation from Kim and O'Neil (1997) are also shown.

$$1,000 \ln \alpha_{(\text{Calcite}-\text{H2O})} = 18.03\left(10^3 T^{-1}\right) - 32.42 \quad (1)$$

where T is in kelvin and α is the fractionation factor. Values produced by Equation 1 are determined relative to the VSMOW scale, and were subsequently converted to the PDB scale for direct comparison to the measured $\delta^{18}O_{FORAM}$ values using the following equation from Coplen et al. (1983):

$$\delta^{18}O(‰\ \text{PDB}) = 0.97002 \times \delta^{18}O(‰\ \text{VSMOW}) - 29.98 \quad (2)$$

Most paleoceanographic studies utilizing *N. pachyderma* use either the Kim and O'Neil (1997) or O'Neil et al. (1969) equations (Kozdon et al., 2009), thus the Kim and O'Neil (1997) equation was employed to reconstruct predicted equilibrium calcite oxygen isotope values shown herein.

3. Results

3.1. Whole-Shell and Individual Chamber TE Differences

Mg/Ca values were similar in the crusted and uncrusted shells, both in their whole-shell and individual chamber distributions (Figure 4a). Zn/Ca ratios also displayed overlapping distributions between the two populations, however, the distributions of values for the uncrusted shells were skewed to higher values than the distributions derived from the crusted shells (Figure 4f). Only Zn/Ca values from the F3 chamber were found to be significantly different between the crusted and uncrusted populations.

The four remaining elemental ratios, Ba/Ca, Na/Ca, Mn/Ca, and Sr/Ca, all show distinct differences between the crusted and uncrusted shells. The uncrusted shells record significantly higher TE/Ca compositions compared to the crusted shells (Figure 4). When observing TE/Ca differences in individual chambers, significant differences between the crusted and uncrusted shells are also found; however, these differences tend to increase in sequentially older chambers. For example, the Sr/Ca difference between the uncrusted and crusted population means increase from 0.011 mmol/mol to 0.031 mmol/mol to 0.075 mmol/mol to 0.080 mmol/mol for the F0, F1, F2, and F3 chambers, respectively (Figure 4e). A similar increase is observed in Ba/Ca, Na/Ca, and Mn/Ca. All Ba/Ca (Figure 4b) and Na/Ca (Figure 4c) chamber populations were statistically different between the crusted and uncrusted shells. The F1, F2, and F3 chambers recorded significant differences in Sr/Ca, and the F2 and F3

chambers recorded significant differences in Mn/Ca. Statistically significant differences were determined using a Mann-Whitney test (p-values < 0.05) and are marked with an asterisk (Figure 4).

3.2. Intrashell Trace Element Variability

Distributions of $\Delta TE/Ca_{inner\text{-}outer}$ values (where $\Delta TE/Ca_{inner\text{-}outer} = Avg(TE/Ca)_{inner50\%} - Avg(TE/Ca)_{outer50\%}$) provide insight into how the crusted and uncrusted intrashell geochemistry differ on three fronts: (a) $\Delta TE/Ca_{inner\text{-}outer}$ show if a portion (i.e., inner 50% or outer 50%) of the shell wall is more enriched in a TE compared to the remainder of the shell wall, (b) the magnitude of TE enrichment within a portion of the shell wall as identified by distributions of $\Delta TE/Ca_{inner\text{-}outer}$ values can be compared between crusted and uncrusted populations, and (c) the chamber-to-chamber variability in $\Delta TE/Ca_{inner\text{-}outer}$ values can be examined. Here, we will review each of these results for the examined analytes. Differences between distributions will be described primarily via a comparison of the innermost quartile ranges.

Differences in Mg/Ca between the inner and outer calcite ($\Delta Mg/Ca_{inner\text{-}outer}$) tend to be minimal for the uncrusted shells, as indicated by the overlap of $\Delta TE/Ca_{inner\text{-}outer}$ distributions with the line of equality or "0" line. In contrast, the crusted shells consistently have positive $\Delta Mg/Ca_{inner\text{-}outer}$ values that increase in progressively older chambers (Figure 6a). Both the crusted and uncrusted *N. pachyderma* shells have enriched Ba/Ca values in the inner calcite, though the $\Delta Ba/Ca_{inner\text{-}outer}$ values tend to deviate farther from the line of equality in crusted shells (Figure 6b). Nearly all chambers show higher Na/Ca in the inner chamber calcite in both crusted and uncrusted shells, as proven by the distinctly positive $\Delta TE/Ca_{inner\text{-}outer}$ distributions (Figure 6c). Only the F0 chamber in the uncrusted shells lacks a $\Delta Na/Ca_{inner\text{-}outer}$ difference. The $\Delta Na/Ca_{inner\text{-}outer}$ values increases markedly in sequentially older chambers. There is only a slight $\Delta Mn/Ca_{inner\text{-}outer}$ difference in uncrusted shells (Figure 6d). Conversely, crusted shells have a positive $\Delta Mn/Ca_{inner\text{-}outer}$ difference in all chambers. The $\Delta Sr/Ca_{inner\text{-}outer}$ values show chamber-to-chamber patterns like those observed with Na/Ca, where $\Delta Sr/Ca_{inner\text{-}outer}$ values increase in progressively older chambers in both the crusted and uncrusted shells (Figures 6c and 6e). However, differences in the distribution of $\Delta Sr/Ca_{inner\text{-}outer}$ values between the youngest (F0) and oldest (F3) chambers is greater among the alive, uncrusted shells when compared to the crusted shells. The F0 and F1 chambers of the uncrusted shells tend to record similar Sr/Ca in the inner and outer halves of the shell wall, whereas the F2 and F3 chambers tend to record higher Sr/Ca in the inner chamber wall. Crusted shells show slight Sr/Ca enrichment in the outer calcite in the F0 chamber and Sr/Ca enrichment in the inner calcite in the F1, F2, and F3 chambers. Zn/Ca is higher in the inner shell wall of both crusted and uncrusted shells; however, crusted shells record consistently more positive $\Delta Zn/Ca_{inner\text{-}outer}$ values than their uncrusted counterparts (Figure 6f). Chamber-to-chamber variability in Zn/Ca is minimal.

The inner 50% of the crusted specimens, primarily composed of early ontogenetic calcite, should be most similar in composition to the uncrusted specimens, which are composed of only early ontogenetic calcite, with little or no crust calcite. A comparison of uncrusted whole-shell TE/Ca data to the TE/Ca data from the inner 50% of the crusted shells demonstrates this similarity (Figure 7). For most TEs, the TE/Ca distributions of the inner 50% of the crusted shells are statistically similar to the TE/Ca distributions of the uncrusted, whole-shell values. Conversely, the outer 50% of the dead, crusted shells are significantly different than the alive, uncrusted shells, recording consistently lower TE concentrations. Only in the case of Sr/Ca are both the crusted inner 50% and outer 50% values significantly different than the uncrusted, whole-shell values (Figure 7c).

3.3. Stable Isotope ($\delta^{13}C$ and $\delta^{18}O$) Differences Between Crusted and Uncrusted Shell Populations

Uncrusted shells generally record higher carbon isotope values and lower oxygen isotope values compared to the crusted shells retrieved from the surface ocean environment (Figure 8). Carbon isotope values for the alive, uncrusted shells range from 0.63‰ to −0.07‰ with an average value of 0.25‰ whereas $\delta^{13}C$ values for the dead, crusted shells range from 0.29‰ to −0.28‰ with an average of −0.05‰ (Figure 8a). Oxygen isotope values range from 0.56‰ to −0.14‰ for uncrusted shells, with an average of 0.12‰, and values range from 0.89‰ to 0.06‰ for crusted shells, with an average of 0.37‰ (Figure 8b). Differences in isotopic composition between the crusted and uncrusted shells are statistically significant for both $\delta^{13}C$ and $\delta^{18}O$ (Student's t-test; $\delta^{13}C$, p-value << 0.001).

4. Discussion

4.1. Trace Element Variability in Crusted and Uncrusted Specimens

The whole-shell average Ba/Ca, Na/Ca, Mn/Ca, and Sr/Ca are significantly higher in the uncrusted shells of *N. pachyderma* compared to crusted shells recovered from the same surface ocean plankton tows (Figures 4b–4e).

Inner calcite TE enrichment (i.e., more positive $\Delta TE/Ca_{inner\text{-}outer}$) is present in both crusted and uncrusted shells but is more pronounced in the crusted specimens (Figure 6). Mg/Ca and Zn/Ca are not significantly different in the uncrusted versus crusted specimens, but the range of values recorded in uncrusted shells is skewed toward higher ratios compared to the crusted shells (Figures 4a and 4f). Comparison of the outer 50% spectral averages (i.e., dominantly crust calcite) to whole-shell uncrusted TE values show a significant TE depletion in the crust calcite (Figure 7). Thus, differences in whole-shell trace element geochemistry, and the positive $\Delta TE/Ca_{inner\text{-}outer}$ values, are attributed to the low TE-bearing crust calcite, which lowers the overall whole-shell average TE/Ca ratios (Figure 6). The crust, which tends to grow thicker on the progressively older chambers, is also likely responsible for the larger $\Delta TE/Ca_{inner\text{-}outer}$ differences in progressively older chambers (e.g., Figures 4b–4e and 6; Fehrenbacher et al., 2017; Sadekov et al., 2005).

High-resolution analyses from fossil specimens demonstrate that nearly all TEs in early ontogenetic calcite are elevated compared to crusted calcite whereas the outer crust is generally more homogeneous, with overall lower trace element ratios (Hathorne et al., 2009; Jonkers et al., 2016; Sadekov et al., 2005; Steinhardt et al., 2015; Table 1). The ontogenetic TE-enriched calcite often appears "banded," with alternating high and low intercalated calcite "layers" (Bonnin et al., 2019; Hathorne et al., 2009; Sadekov et al., 2005; Steinhardt et al., 2015). The higher ratios of these elements in the innermost chamber walls could be related to the presence of organic layers embedded in the shell wall that form with chamber growth and thickening processes. Chamber formation processes are variable amongst different species but share a common feature: as the chambers are added and/or thickened during early ontogeny, organic membranes form between the thin calcite layers. The initial calcite that forms adjacent to the organic membrane is often enriched in TEs (Bonnin et al., 2019; Cuif et al., 2012; Fehrenbacher et al., 2017; Richey et al., 2022). The mechanism responsible for the enriched TEs associated with the organic membranes is poorly constrained but may be linked to processes responsible for nucleating calcite on the organic templates (Branson et al., 2019).

The higher ratios in the inner calcite could also reflect variable conditions in the microhabitat surrounding the shells during early ontogeny. The microhabitat is a complicated space that has remarkably different chemistry compared to the adjacent seawater (Jørgensen et al., 1985; Rink et al., 1998). First, foraminifera respire, which likely modulates the carbonate chemistry and oxygen concentration in the microenvironment around their shells. Studies have also demonstrated that foraminifera increase the pH in the microenvironment during chamber formation (de Nooijer et al., 2008, 2009). For species with algal symbionts, the changes in pH and oxygen are even more pronounced due to diurnal algal photosynthesis cycles (Jørgensen et al., 1985; Köhler-Rink & Kühl, 2000). While our study species is asymbiotic and thus is not affected by photosynthetic cycles, there is growing evidence that nonspinose foraminifera, including *N. pachyderma*, calcify within a particulate organic microhabitat, such as marine snow, during early ontogeny (Fehrenbacher et al., 2018; Fritz-Endres et al., 2022; Greco et al., 2019; Richey et al., 2022). Marine snow can have highly variable pH, oxygen concentrations, and even different seawater trace element compositions (Alldredge & Cohen, 1987; Hebel et al., 1986). During periods of high productivity, calcification within marine snow can be more common, resulting in higher Ba/Ca ratios among nonspinose foraminifera (Fritz-Endres et al., 2022). However, the specimens examined in this study were captured during a period of relatively low productivity (i.e., chlorophyll a <0.25 mg/m^3; Figure 3) and so we do not find high Ba/Ca compositions like those observed in other studies of nonspinose foraminifera (Fehrenbacher et al., 2017; Richey et al., 2022). Although the exact mechanism responsible for differences in the geochemistry of the early ontogenetic calcite and the outer crust is not well constrained, results herein confirm that the inner calcite of *N. pachyderma* has consistently enriched TEs whereas the crust calcite consistently records lower trace elements (Figures 4, 6, and 7).

Crust formation remains an enigmatic process (Hamilton et al., 2008). Why are trace elements lower in crust calcite when compared to the early ontogenetic calcite? Moreover, why does the crust lack TE variability? Although it is widely accepted that foraminifera crusting occurs during late ontogeny, and typically during or just prior to gametogenesis, the mechanisms modulating TE incorporation during this process are not well constrained. In the foraminiferal species *Orbulina universa* and *Neogloboquadrina dutertrei*, it has been shown that calcite that forms during the day has lower Mg/Ca ratios compared to calcite that forms at night. If the crust forms rapidly, and during daylight hours, this may be responsible for the low TE composition of the crust calcite (Fehrenbacher et al., 2017; Spero et al., 2015). Culture studies using foraminiferal species that have been shown to generate crust in culture, like *Neogloboquadrina incompta* (Davis et al., 2017), could shed further light on TE incorporation processes during crusting.

Intrashell variability was evaluated by examining chamber-to-chamber variability and $\Delta TE/Ca_{inner\text{-}outer}$ gradients. $\Delta TE/Ca_{inner\text{-}outer}$ gradients were used to determine if the outer crusted calcite recorded relatively lower TE concentrations. While this is a useful tactic to evaluate the general chemical distribution in the crust versus ontogenetic calcite on a population scale, it inherently simplifies the structure of TE variability in the shell wall. For example, in Figure 5a, Zn/Ca is consistently low in the outer 50% of the spectrum whereas it increases to a distinct peak in the inner 50% of the spectrum. The general structure of Zn/Ca observed in Figure 5a supports an idealized view of a "low TE" crust that appears to be clearly distinguishable from the inner ontogenetic calcite. However, Ba/Ca of the same shell (Figure 5b) shows several bands of fluctuating high and low Ba/Ca throughout the entire spectrum, although when calculated the average of the inner 50% of the spectrum is higher than the average of the outer 50%. While these observations do not hinder the interpretations described herein, it is worth noting that intrashell TE variability is simply more complex than the $\Delta TE/Ca_{inner\text{-}outer}$ gradients that were employed to assess it. However, comparison of representative TE/Ca spectra from a crusted specimen and an uncrusted specimen (Figure 5) shows that greater variability is found throughout the depth profile in uncrusted specimens, whereas inner-outer TE differences are generally more visually apparent in crusted specimens.

4.2. Habitat Depth and Crust Formation: Insights From Stable Isotopes

While the planktic foraminiferal life-cycle and preferred habitat depth is an ongoing area of research (e.g., Meilland et al., 2021), it is generally believed that many species of foraminifera undergo gametogenesis and grow the associated crust at depths deeper than their typical, average, living depth habitat (Bauch et al., 2002; Duplessy et al., 1981; Hemleben et al., 1989; Schiebel & Hemleben, 2017). Stable isotope data from the crusted and uncrusted shell populations presented herein support this notion. The uncrusted shells record higher $\delta^{13}C$ values and lower $\delta^{18}O$ values compared to crusted shells acquired from the same plankton tows (Figure 8). These differences suggest that *N. pachyderma* live in the ^{13}C-enriched, warmer waters of the upper surface ocean during early ontogeny and develop the late gametogenic crust deeper in the water column. The relatively cooler temperatures are responsible for the higher $\delta^{18}O$ signature of the crusted specimens while the increase in organic matter decomposition in deeper water lowers the seawater $\delta^{13}C_{DIC}$, thereby also lowering the $\delta^{13}C_{FORAM}$ (i.e., shell) composition. Similar relative differences have been found in isotopic comparisons of crusted and uncrusted shells of both spinose (Blanc & Bé, 1981; Mulitza et al., 1997; Schweitzer & Lohmann, 1991; Vergnaud Grazzini, 1976) and nonspinose (Bauch et al., 2002; Kozdon et al., 2009; Livsey et al., 2020) species.

The $\delta^{13}C$ values recorded by both crusted and uncrusted shells are within the range of $\delta^{13}C_{DIC}$ values measured from the upper water column, suggesting that the *N. pachyderma* examined herein were collected during a low productivity period and grew their shells in equilibrium with seawater $\delta^{13}C_{DIC}$. A similar observation is made when comparing the $\delta^{18}O_{FORAM}$ population distribution to the $\delta^{18}O$ profile of predicted equilibrium calcite (Figures 8 and 9). We therefore argue that comparisons between shell and water isotope geochemistry can be used to make inferences about the living depth habitat and depth of crusting (Figure 9). The uncrusted $\delta^{13}C_{FORAM}$ values suggest that these foraminifera calcified between ~45 and 85 m below the surface during their lifetime. The distribution of the crusted shells aligns with $\delta^{13}C_{DIC}$ signatures found at depths of ~73–102 m. However, crusted shells are a mixture of ontogenetic calcite and crust calcite. If we assume that the average $\delta^{13}C$ value of the living shell distribution is representative of the ontogenetic calcite shell ($\delta^{13}C_{onto} = 0.24‰$) and use the average $\delta^{13}C$ value of the crusted shells as our "mixed" signature ($\delta^{13}C_{crusted} = -0.05‰$), we can determine potential crusting depths by modeling various scenarios of % crust and % ontogenetic calcite (Figure 9a). For example, if the crusted shells were a mixture of 70% crust calcite and 30% ontogenetic calcite, the crust calcite would need to have been added at a depth of ~92 m where the $\delta^{13}C_{DIC}$ is −0.17‰. Conversely, if crusted shells were composed of 40% crust calcite and 60% ontogenetic calcite, the crust would need to be added near a depth of ~227 m where the $\delta^{13}C_{DIC}$ is −0.49‰. A 30% crust calcite/70% ontogenetic calcite mixture would require the crust calcite end-member to have a $\delta^{13}C$ signature of −0.73‰ which is below the minimum $\delta^{13}C_{DIC}$ values recorded in the upper 500 m of the water column. These mixing scenarios, in combination with the fact that all shells were collected from the uppermost 200 m of the water column, suggest that shells are composed of between 40% and 70% crust calcite, and that crusting likely occurs between ~100 and 200 m below the surface. Estimates of crust volume interpreted here are consistent with SEM imaging of shell cross sections and mass-balance calculations derived from weight comparisons of crusted and uncrusted shells where the crust calcite has been found to compose anywhere from ~30% to 70% of the total shell volume (Bauch et al., 2002; Bé, 1980; Bolton & Marr, 2013; Mulitza et al., 1997). The depth of crusting determined herein is also consistent with observations of *N. pachyderma* from plankton tow studies in

the Okhotsk Sea (Bauch et al., 2002) but is shallower then crusting depths found in the Labrador Sea, Greenland Sea, and Fram Strait (~200–400 m; Kozdon et al., 2009; Stangeew, 2001). Studies of *N. pachyderma* populations throughout the Arctic have found depth habitats (calculated as the abundance-weighted mean depth determined using the midpoints of the collection intervals) ranging from 25 to 280 m water depth (Greco et al., 2019). Sparse depth-stratified assemblage data published for the study region (Ortiz et al., 1996) have found specimens living dominantly within the upper 200 m of the water column, with shells found below 200 m representing a settling flux of dead shells. The variable depth at which crust forms is likely driven simply by hydrographic conditions, which will differ across study regions.

Comparisons of the $\delta^{18}O_{FORAM}$ range to the $\delta^{18}O$ profile predicted from calcification at equilibrium with seawater produces an estimated living depth habitat of ~30–68 m. If we employ a similar mixing model approach using the average $\delta^{18}O$ of the uncrusted shells ($\delta^{18}O_{onto}$= 0.08‰) as the ontogenetic calcite end-member and the average $\delta^{18}O$ of the crusted shells as the "mixed" signature, crusting mixtures of ≥20% provide reasonable crusting depths near or within the uppermost 200 m of the water column.

While the $\delta^{13}C$ mixing model provides a first approximation of crusting depths, it is possible that the foraminiferal calcite may not be directly recording the $\delta^{13}C_{DIC.}$ Isotopic investigations of *N. pachyderma* from the Okhotsk Sea have recognized offsets between $\delta^{13}C_{DIC}$ and $\delta^{13}C_{shell}$ that were attributed to grow under lower carbonate ion concentrations (i.e., the "carbonate ion effect" (Bauch et al., 2002; Spero et al., 1997)). However, consistency in the interpreted living depth habitats interpolated from both the $\delta^{13}C$ and $\delta^{18}O$ shell distributions provides some confidence that the foraminiferal $\delta^{13}C$ is not strongly affected by carbonate ion concentration in our study region.

4.3. Crusting in Planktic Foraminifera: Implications for Paleoreconstruction

Intrashell TE variability has been widely explored in many planktic foraminiferal species using an array of techniques including LA-ICP-MS and electron microprobe mapping, among others (Table 1 and references therein). Together, this body of literature suggests that for most planktic foraminiferal taxa the crust portions of foraminiferal shells tend to record lower trace elements, leading to overall lower whole-shell trace element concentrations in crusted shells. These previous studies have generally focused on Mg/Ca variability and evaluations derived from a few individuals. Here, we expand the investigated elements and work to constrain patterns observed consistently in a larger population to better understand trace element incorporation for a single, critically important foraminiferal species. Population-scale geochemical TE/Ca variability, statistically robust evaluations of intrashell variability, and associated differences between crusted and uncrusted shell populations collected from the same plankton tows in the upper surface ocean demonstrate how shell geochemistry changes in association with gametogenic crust formation. Results serve as a baseline for comparison to regional sediment trap and core-top studies to better delineate geochemical changes that occur between initial calcification in the water column and fossilization on the seafloor.

A few observations presented herein deviate from precursor studies. While Mg/Ca has been found to generally be lower in crust calcite when compared to ontogenetic calcite for most taxa (Table 1), we do not find significant differences when comparing Mg/Ca values derived from uncrusted and crusted shells of *N. pachyderma* (Figures 4a and 6a). Significant differences in Mg/Ca are found when comparing the outer 50% of the crusted shells to the uncrusted whole-shell values (Figure 7a), but the translation of these differences into whole-shell values does not appear to produce a vital effect that would affect temperature estimates derived from these shells. The small differences in Mg/Ca between the crust and ontogenetic portions of the shells may be supportive of either (a) interpretation that these shells are minimally crusted or conversely, (b) that crusting is occurring over a small temperature gradient between living depth and crusting depth. Specimens that calcify when there is a larger temperature gradient over the depth habitat range may have larger Mg/Ca differences in ontogenetic versus crust calcite. It has also been argued that the depth of crusting varies for a foraminifer following gametogenesis, as interpreted by chamber-to-chamber differences observed in Mg/Ca in studies of *N. dutertrei* (Jonkers et al., 2012). Yet TE/Ca content in crusted specimens of *N. pachyderma* examined in this study record very similar Mg/Ca distributions in the penultimate and preceding chambers (i.e., F1–F3 chambers; Figure 4) suggesting rapid crust development occurring at a consistent depth. Although we do not find distinct differences in Mg/Ca between crusted and uncrusted individuals collected via plankton tow, there is a potential for Mg/Ca alteration of shells to occur while settling through the water column and/or upon deposition to the seafloor (Dekens et al., 2002; Sadekov et al., 2010; Wycech et al., 2016). Precipitation of secondary diagenetic calcite at lower temperatures,

such as those found along the seafloor, would further increase the relative volume of low-Mg calcite in the shells of fossil foraminifers.

There is growing interest in understanding mechanisms responsible for the incorporation of the elements Na, Mn, Zn, and Ba, because of their potential utility in paleoclimate as proxies for salinity, oxygenation, water mass tracing, and paleoproductivity, respectively (Bertlich et al., 2018; Bryan & Marchitto, 2010; Fehrenbacher et al., 2018; Fritz-Endres et al., 2022; Marchitto et al., 2000; Mezger et al., 2016; Steinhardt et al., 2014; Watkins et al., 2021; Wit et al., 2013). For *N. pachyderma*, results herein demonstrate that these elements are highly variable in the early ontogenetic calcite and that the crust calcite has overall lower TE/Ca ratios. Culture experiments remain invaluable for understanding mechanisms responsible for the incorporation of these elements. However, for species that form crusts, crusted plankton tow, sediment trap, and seafloor specimens may be better suited for the generation of TE-environment calibrations that can be applied to downcore reconstructions. Depending on the region, crusted shells are more likely to be preserved in the fossil record (Caron et al., 1990; Johnstone et al., 2010), and thus in these cases, calibrations to appropriately assess their geochemistry should be prioritized.

5. Conclusions

Culturing studies of foraminifera have been invaluable to the field of paleoceanographic proxy development (Schiebel & Hemleben, 2017); however, culturing of planktic foraminifera is not without its hardships. Previous culturing studies of neogloboquadrinids have noted difficulty in getting foraminifera to develop thick crusts similar to those found in nature (Davis et al., 2017; Fehrenbacher et al., 2017). Here, we examine trace element (Mg/Ca, Na/Ca, Sr/Ca, Ba/Ca, Mn/Ca, Zn/Ca) and stable isotope ($\delta^{13}C$, $\delta^{18}O$) geochemistry of crusted and uncrusted shells of *N. pachyderma* collected from the same surface ocean plankton tows to investigate potential vital effects associated with the development of gametogenic crusts. Results herein show that for most TEs (Na, Sr, Ba, Mn), TE/Ca values are significantly higher in uncrusted shells when compared to crusted shells. Whole-shell TE values are lower for crusted shells due to the inclusion of low TE-bearing crust. Stable isotope comparisons of foraminiferal shells to ambient seawater indicate that *N. pachyderma* live within the uppermost 90 m of the water column. We have estimated that the crust composes ∼40%–70% of the shell volume in crusted shells, and that crusting occurs between ∼100 and 200 m water depth. If TE/Ca culture calibrations are established from TE-enriched uncrusted or weakly crusted shells and applied to crusted fossil shells, the associated paleoreconstructions will inherently produce attenuated climate signals. We therefore recommend (a) using calibrations established from crusted specimens to evaluate fossil records; or (b) that calibrations based on ontogenetic calcite should be only applied to the ontogenetic portions of fossil specimens using LA-ICP-MS profiling, as previously suggested by Davis et al. (2017).

Data Availability Statement

All data referenced herein are available from the Dryad Data Repository at Hupp and Fehrenbacher (2023).

Acknowledgments
This research was supported by the NOAA Climate and Global Change Postdoctoral Fellowship Program, administered by UCAR's Cooperative Programs for the Advancement of Earth System Science (CPAESS) under Award #NA21OAR4310383. This work was further supported an NSF OCE Grant 2222365 to B.H. and J.F. and NSF OCE 2049143 to J.F. Special thanks to the crew and science party of the May 2022 NCC Bell M. Shimada Cruise and the Oregon State University Keck Plasma Laboratory and Stable Isotope Laboratory. We also thank NOAA-Fisheries for the ship time that supported data collection for this research.

References

Alldredge, A., & Cohen, Y. (1987). Can microscale chemical patches persist in the sea? Microelectrode study of marine snow, fecal pellets. *Science*, *235*, 689–691. https://doi.org/10.1126/science.235.4789.689

Allen, K. A., Hönisch, B., Eggins, S. M., Haynes, L. L., Rosenthal, Y., & Yu, J. (2016). Trace element proxies for surface ocean conditions: A synthesis of culture calibrations with planktic foraminifera. *Geochimica et Cosmochimica Acta*, *193*, 197–221. https://doi.org/10.1016/j.gca.2016.08.015

Anand, P., Elderfield, H., & Conte, M. H. (2003). Calibration of Mg/Ca thermometry in planktonic foraminifera from a sediment trap time series: Calibration of Mg/Ca thermometry in planktonic foraminifera. *Paleoceanography*, *18*(2), 1050. https://doi.org/10.1029/2002PA000846

Bauch, D., Erlenkeuser, H., Winckler, G., Pavlova, G., & Thiede, J. (2002). Carbon isotopes and habitat of polar planktic foraminifera in the Okhotsk Sea: The 'carbonate ion effect' under natural conditions. *Marine Micropaleontology*, *45*, 83–99. https://doi.org/10.1016/S0377-8398(02)00038-5

Bé, A. W. H. (1980). Gametogenic calcification in a spinose planktonic foraminifer, *Globigerinoides sacculifer* (Brady). *Marine Micropaleontology*, *5*, 283–310. https://doi.org/10.1016/0377-8398(80)90014-6

Bé, A. W. H., & Lott, L. (1964). Shell growth and structure of planktonic foraminifera. *Science*, *145*(3634), 823–824. https://doi.org/10.1126/science.145.3634.823

Bertlich, J., Nürnberg, D., Hathorne, E. C., de Nooijer, L. J., Mezger, E. M., Kienast, M., et al. (2018). Salinity control on Na incorporation into calcite tests of the planktonic foraminifera *Trilobatus sacculifer*—Evidence from culture experiments and surface sediments. *Biogeosciences*, *15*(20), 5991–6018. https://doi.org/10.5194/bg-15-5991-2018

Blanc, P.-L., & Bé, A. W. H. (1981). Oxygen-18 enrichment of planktonic foraminifera due to gametogenic calcification below the euphotic zone. *Science*, *213*(4513), 1247–1250. https://doi.org/10.1126/science.213.4513.1247

Bolton, A., & Marr, J. P. (2013). Trace element variability in crust-bearing and non-crust-bearing *Neogloboquadrina incompta*, P-D intergrade and *Globoconella inflata* from the Southwest Pacific Ocean: Potential paleoceanographic implications. *Marine Micropaleontology*, *100*, 21–33. https://doi.org/10.1016/j.marmicro.2013.03.008

Bonnin, E. A., Zhu, Z., Fehrenbacher, J. S., Russell, A. D., Hönisch, B., Spero, H. J., & Gagnon, A. C. (2019). Submicron sodium banding in cultured planktic foraminifera shells. *Geochimica et Cosmochimica Acta*, *253*, 127–141. https://doi.org/10.1016/j.gca.2019.03.024

Branson, O., Fehrenbacher, J. S., Vetter, L., Sadekov, A. Y., Eggins, S. M., & Spero, H. J. (2019). LAtools: A data analysis package for the reproducible reduction of LA-ICPMS data. *Chemical Geology*, *504*, 83–95. https://doi.org/10.1016/j.chemgeo.2018.10.029

Branson, O., Read, E., Redfern, S. A. T., Rau, C., & Elderfield, H. (2015). Revisiting diagenesis on the Ontong Java plateau: Evidence for authigenic crust precipitation in *Globorotalia tumida*. *Paleoceanography*, *30*, 1490–1502. https://doi.org/10.1002/2014PA002759

Brown, S. J., & Elderfield, H. (1996). Variations in Mg/Ca and Sr/Ca ratios of planktonic foraminifera caused by post depositional dissolution: Evidence of shallow Mg-dependent dissolution. *Paleoceanography*, *11*, 543–551. https://doi.org/10.1029/96PA01491

Bryan, S. P., & Marchitto, T. M. (2010). Testing the utility of paleonutrient proxies Cd/Ca and Zn/Ca in benthic foraminifera from thermocline waters: Cd/Ca and Zn/Ca in benthic foraminifera. *Geochemistry, Geophysics, Geosystems*, *11*, Q01005. https://doi.org/10.1029/2009GC002780

Caron, D. A., Roger Anderson, O., Lindsey, J. L., Faber, W. W., & Lin Lim, E. E. (1990). Effects of gametogenesis on test structure and dissolution of some spinose planktonic foraminifera and implications for test preservation. *Marine Micropaleontology*, *16*(1–2), 93–116. https://doi.org/10.1016/0377-8398(90)90031-G

Coplen, T. B., Kendall, C., & Hopple, J. (1983). Comparison of stable isotope reference samples. *Nature*, *302*(5905), 236–238. https://doi.org/10.1038/302236a0

Cuif, J.-P., Dauphin, Y., Nehrke, G., Nouet, J., & Perez-Huerta, A. (2012). Layered growth and crystallization in calcareous biominerals: Impact of structural and chemical evidence on two major concepts in Invertebrate biomineralization studies. *Minerals*, *2*(1), 11–39. https://doi.org/10.3390/min2010011

Davis, C. V., Fehrenbacher, J. S., Benitez-Nelson, C., & Thunell, R. C. (2020). Trace element heterogeneity across individual planktic foraminifera from the modern Cariaco Basin. *Journal of Foraminiferal Research*, *50*(2), 204–218. https://doi.org/10.2113/gsjfr.50.2.204

Davis, C. V., Fehrenbacher, J. S., Hill, T. M., Russell, A. D., & Spero, H. J. (2017). Relationships between temperature, pH, and crusting on Mg/Ca ratios in laboratory-grown *Neogloboquadrina* foraminifera: Mg/Ca in *Neogloboquadrina foraminifera*. *Paleoceanography*, *32*, 1137–1152. https://doi.org/10.1002/2017PA003111

Dekens, P. S., Lea, D. W., Pak, D. K., & Spero, H. J. (2002). Core top calibration of Mg/Ca in tropical foraminifera: Refining paleotemperature estimation: Core top calibration. *Geochemistry, Geophysics, Geosystems*, *3*(4), 1–29. https://doi.org/10.1029/2001GC000200

De Nooijer, L. J., Toyofuku, T., & Kitazato, H. (2009). Foraminifera promote calcification by elevating their intracellular pH. *Proceedings of the National Academy of Sciences of the United States of America*, *106*(36), 15374–15378. https://doi.org/10.1073/pnas.0904306106

De Nooijer, L. J., Toyofuku, T., Oguri, K., Nomaki, H., & Kitazato, H. (2008). Intracellular pH distribution in Foraminifera determined by the fluorescent probe HPTS. *Limnology and Oceanography: Methods*, *6*(11), 610–618. https://doi.org/10.4319/lom.2008.6.610

Duckworth, D. L. (1977). Magnesium concentration in the tests of the planktonic foraminifer *Globorotalia truncatulinoides*. *Journal of Foraminiferal Research*, *7*(4), 304–312. https://doi.org/10.2113/gsjfr.7.4.304

Duplessy, J. C., Bé, A. W. H., & Blanc, P. L. (1981). Oxygen and carbon isotopic composition and biogeographic distribution of planktonic foraminifera in the Indian Ocean. *Palaeogeography, Palaeoclimatology, Palaeoecology*, *33*(1–3), 9–46. https://doi.org/10.1016/0031-0182(81)90031-6

Eggins, S., De Deckker, P., & Marshall, J. (2003). Mg/Ca variation in planktonic foraminifera tests: Implications for reconstructing palaeo-seawater temperature and habitat migration. *Earth and Planetary Science Letters*, *212*(3–4), 291–306. https://doi.org/10.1016/S0012-821X(03)00283-8

Elderfield, H., & Ganssen, G. (2000). Past temperature and $\delta^{18}O$ of surface ocean waters inferred from foraminiferal Mg/Ca ratios. *Nature*, *405*(6785), 442–445. https://doi.org/10.1038/35013033

Fehrenbacher, J. S., Russell, A. D., Davis, C. V., Gagnon, A. C., Spero, H. J., Cliff, J. B., et al. (2017). Link between light-triggered Mg-banding and chamber formation in the planktic foraminifera *Neogloboquadrina dutertrei*. *Nature Communications*, *8*(1), 15441. https://doi.org/10.1038/ncomms15441

Fehrenbacher, J. S., Russell, A. D., Davis, C. V., Spero, H. J., Chu, E., & Hönisch, B. (2018). Ba/Ca ratios in the non-spinose planktic foraminifer *Neogloboquadrina dutertrei*: Evidence for an organic aggregate microhabitat. *Geochimica et Cosmochimica Acta*, *236*, 361–372. https://doi.org/10.1016/j.gca.2018.03.008

Fritz-Endres, T., Fehrenbacher, J. S., Russell, A. D., & Cynar, H. (2022). Increased productivity in the equatorial pacific during the deglaciation inferred from the Ba/Ca ratios of non-spinose planktic foraminifera. *Paleoceanography and Paleoclimatology*, *37*, e2022PA004506. https://doi.org/10.1029/2022PA004506

Greco, M., Jonkers, L., Kretschmer, K., Bijma, J., & Kucera, M. (2019). Depth habitat of the planktonic foraminifera *Neogloboquadrina pachyderma* in the northern high latitudes explained by sea-ice and chlorophyll concentrations. *Biogeosciences*, *16*(17), 3425–3437. https://doi.org/10.5194/bg-16-3425-2019

Hamilton, C. P., Spero, H. J., Bijma, J., & Lea, D. W. (2008). Geochemical investigation of gametogenic calcite addition in the planktonic foraminifera *Orbulina universa*. *Marine Micropaleontology*. *Marine Micropaleontology*, *68*(3), 256–267. https://doi.org/10.1016/j.marmicro.2008.04.003

Hathorne, E. C., James, R. H., & Lampitt, R. S. (2009). Environmental versus biomineralization controls on the intratest variation in the trace element composition of the planktonic foraminifera *G. inflata* and *G. scitula*: Environmental versus biomineral controls. *Paleoceanography*, *24*, PA4204. https://doi.org/10.1029/2009PA001742

Hebel, D., Knauer, G. A., & Martin, J. H. (1986). Trace-metals in large agglomerates (marine snow). *Journal of Plankton Research*, *8*(4), 819–824. https://doi.org/10.1093/plankt/8.4.819

Hemleben, C., Spindler, M., & Anderson, O. R. (1989). *Modern planktonic foraminifera* (pp. 363). Springer.

Hönisch, B., Allen, K. A., Lea, D. W., Spero, H. J., Eggins, S. M., Arbuszewski, J., et al. (2013). The influence of salinity on Mg/Ca in planktic foraminifers—Evidence from cultures, core-top sediments and complementary $\delta^{18}O$. *Geochimica et Cosmochimica Acta*, *121*, 196–213. https://doi.org/10.1016/j.gca.2013.07.028

Hupp, B., & Fehrenbacher, J. (2023). *Neogloboquadrina pachyderma* LA-ICP-MS spectral files and stable isotopes data from "Geochemical differences between alive, uncrusted and dead, crusted shells of *Neogloboquadrina pachyderma*: Implications for paleoreconstruction" [Dataset]. Dryad. https://doi.org/10.5061/dryad.gtht76hsk

Jochum, K. P., Weis, U., Stoll, B., Kuzmin, D., Yang, Q., Raczek, I., et al. (2011). Determination of reference values for NIST SRM 610-617 glasses following ISO guidelines. *Geostandards and Geoanalytical Research*, *35*(4), 397–429. https://doi.org/10.1111/j.1751-908X.2011.00120.x

Johnstone, H. J. H., Schulz, M., Barker, S., & Elderfield, H. (2010). Inside story: An X-ray computed tomography method for assessing dissolution in the tests of planktonic foraminifera. *Marine Micropaleontology*, *77*(1–2), 58–70. https://doi.org/10.1016/j.marmicro.2010.07.004

Jonkers, L., Buse, B., Brummer, G.-J. A., & Hall, I. R. (2016). Chamber formation leads to Mg/Ca banding in the planktonic foraminifer *Neogloboquadrina pachyderma*. *Earth and Planetary Science Letters*, *451*, 177–184. https://doi.org/10.1016/j.epsl.2016.07.030

Jonkers, L., de Nooijer, L. J., Reichart, G.-J., Zahn, R., & Brummer, G.-J. A. (2012). Encrustation and trace element composition of *Neogloboquadrina dutertrei* assessed from single chamber analyses—Implications for paleotemperature estimates. *Biogeosciences*, *9*(11), 4851–4860. https://doi.org/10.5194/bg-9-4851-2012

Jørgensen, B. B., Erez, J., Revsbech, P., & Cohen, Y. (1985). Symbiotic photosynthesis in a planktonic foraminiferan, *Globigerinoides sacculifer* (Brady), studied with microelectrodes 1. *Limnology & Oceanography*, *30*(6), 1253–1267. https://doi.org/10.4319/lo.1985.30.6.1253

Katz, M. E., Cramer, B. S., Franzese, A., Hönisch, B., Miller, K. G., Rosenthal, Y., & Wright, J. D. (2010). Traditional and emerging geochemical proxies in foraminifera. *Journal of Foraminiferal Research*, *40*(2), 165–192. https://doi.org/10.2113/gsjfr.40.2.165

Kim, S.-T., & O'Neil, J. R. (1997). Equilibrium and nonequilibrium oxygen isotope effects in synthetic carbonates. *Geochimica et Cosmochimica Acta*, *61*(16), 3461–3475. https://doi.org/10.1016/S0016-7037(97)00169-5

Köhler-Rink, S., & Kühl, M. (2000). Microsensor studies of photosynthesis and respiration in larger symbiotic foraminifera. I The physico-chemical microenvironment of *Marginopora vertebralis*, *Amphistegina lobifera* and *Amphisorus hemprichii*. *Marine Biology*, *137*(3), 473–486. https://doi.org/10.1007/s002270000335

Kozdon, R., Ushikubo, T., Kita, N. T., Spicuzza, M., & Valley, J. W. (2009). Intratest oxygen isotope variability in the planktonic foraminifer *N. pachyderma*: Real vs. apparent vital effects by ion microprobe. *Chemical Geology*, *258*(3–4), 327–337. https://doi.org/10.1016/j.chemgeo.2008.10.032

Lane, M. K., Fehrenbacher, J. S., Fisher, J. L., Fewings, M. R., Crump, B. C., Risien, C. M., et al. (2023). Planktonic foraminiferal assemblages reflect warming during two recent mid-latitude marine heatwaves. *Frontiers in Marine Science*, *10*, 1155761. https://doi.org/10.3389/fmars.2023.1155761

Lea, D. W., Mashiotta, T. A., & Spero, H. J. (1999). Controls on magnesium and strontium uptake in planktonic foraminifera determined by live culturing. *Geochimica et Cosmochimica Acta*, *63*(16), 2369–2379. https://doi.org/10.1016/S0016-7037(99)00197-0

Livsey, C. M., Kozdon, R., Bauch, D., Brummer, G.-J. A., Jonkers, L., Orland, I., et al. (2020). High-resolution Mg/Ca and $\delta^{18}O$ patterns in modern *Neogloboquadrina pachyderma* from the Fram Strait and Irminger Sea. *Paleoceanography and Paleoclimatology*, *35*, e2020PA003969. https://doi.org/10.1029/2020PA003969

Longerich, H. P., Jackson, S. E., & Günther, D. (1996). Inter-laboratory note. Laser ablation inductively coupled plasma mass spectrometric transient signal data acquisition and analyte concentration calculation. *Journal of Analytical Atomic Spectrometry*, *11*(9), 899–904. https://doi.org/10.1039/ja9961100899

Marchitto, T. M., Curry, W. B., & Oppo, D. W. (2000). Zinc concentrations in benthic foraminifera reflect seawater chemistry. *Paleoceanography*, *15*(3), 299–306. https://doi.org/10.1029/1999PA000420

Martin, P. A., & Lea, D. W. (2002). A simple evaluation of cleaning procedures on fossil benthic foraminiferal Mg/Ca. *Geochemistry, Geophysics, Geosystems*, *3*(10), 1–8. https://doi.org/10.1029/2001GC000280

Martínez-Botí, M. A., Mortyn, P. G., Schmidt, D. N., Vance, D., & Field, D. B. (2011). Mg/Ca in foraminifera from plankton tows: Evaluation of proxy controls and comparison with core tops. *Earth and Planetary Science Letters*, *307*(1–2), 113–125. https://doi.org/10.1016/j.epsl.2011.04.019

Meilland, J., Siccha, M., Kaffenberger, M., Bijma, J., & Kucera, M. (2021). Population dynamics and reproduction strategies of planktonic foraminifera in the open ocean. *Biogeosciences*, *18*(20), 5789–5809. https://doi.org/10.5194/bg-18-5789-2021

Mezger, E. M., de Nooijer, L. J., Boer, W., Brummer, G.-J. A., & Reichart, G.-J. (2016). Salinity controls on Na incorporation in Red Sea planktonic foraminifera. *Paleoceanography*, *31*, 1562–1582. https://doi.org/10.1002/2016PA003052

Mulitza, S., Dürkoop, A., Hale, W., Wefer, G., & Stefan Niebler, H. (1997). Planktonic foraminifera as recorders of past surface-water stratification. *Geology*, *25*(4), 335. https://doi.org/10.1130/0091-7613(1997)025<0335:PFAROP>2.3.CO;2

Niebler, H. S., Hubberten, H. W., & Gersonde, R. (1999). Oxygen isotope values of planktic foraminifera: A tool for the reconstruction of surface water stratification. In G. Fischer, & G. Wefer (Eds.), *Use of proxies in Paleoceanography: Examples from the South Atlantic* (pp. 165–189). Springer.

Nürnberg, D., Bijma, J., & Hemleben, C. (1996). Assessing the reliability of magnesium in foraminiferal calcite as a proxy for water mass temperatures. *Geochimica et Cosmochimica Acta*, *60*(5), 803–814. https://doi.org/10.1016/0016-7037(95)00446-7

O'Neil, J. R., Clayton, R. N., & Mayeda, T. K. (1969). Oxygen isotope fractionation in divalent metal carbonates. *The Journal of Chemical Physics*, *51*(12), 5547–5558. https://doi.org/10.1063/1.1671982

Ortiz, J. D., & Mix, A. C. (1992). The spatial distribution and seasonal succession of planktonic foraminifera in the California Current off Oregon, September 1987–September 1988. *Geological Society, London, Special Publications*, *64*(1), 197–213. https://doi.org/10.1144/GSL.SP.1992.064.01.13

Ortiz, J. D., Mix, A. C., Rugh, W., Watkins, J. M., & Collier, R. W. (1996). Deep-dwelling planktonic foraminifera of the northeastern Pacific Ocean reveal environmental control of oxygen and carbon isotopic disequilibria. *Geochimica et Cosmochimica Acta*, *60*(22), 4509–4523. https://doi.org/10.1016/S0016-7037(96)00256-6

Pena, L. D., Cacho, I., Calvo, E., Pelejero, C., Eggins, S., & Sadekov, A. (2008). Characterization of contaminant phases in foraminifera carbonates by electron microprobe mapping. *Geochemistry, Geophysics, Geosystems*, *9*, Q07012. https://doi.org/10.1029/2008GC002018

Richey, J. N., Fehrenbacher, J. S., Reynolds, C. E., Davis, C. V., & Spero, H. J. (2022). Barium enrichment in the non-spinose planktic foraminifer, *Globorotalia truncatulinoides*. *Geochimica et Cosmochimica Acta*, *333*, 184–199. https://doi.org/10.1016/j.gca.2022.07.006

Rink, S., Kühl, M., Bijma, J., & Spero, H. J. (1998). Microsensor studies of photosynthesis and respiration in the symbiotic foraminifer *Orbulina universa*. *Marine Biology*, *131*(4), 583–595. https://doi.org/10.1007/s002270050350

Rosenthal, Y., Lohmann, G. P., Lohmann, K. C., & Sherrell, R. M. (2000). Incorporation and preservation of Mg in *Globigerinoides sacculifer:* Implications for reconstructing the temperature and $^{18}O/^{16}O$ of seawater. *Paleoceanography*, *15*(1), 135–145. https://doi.org/10.1029/1999PA000415

Russell, A. D., Hönisch, B., Spero, H. J., & Lea, D. W. (2004). Effects of seawater carbonate ion concentration and temperature on shell U, Mg, and Sr in cultured planktonic foraminifera. *Geochimica et Cosmochimica Acta*, *68*(21), 4347–4361. https://doi.org/10.1016/j.gca.2004.03.013

Sadekov, A. Y., Eggins, S. M., & De Deckker, P. (2005). Characterization of Mg/Ca distributions in planktonic foraminifera species by electron microprobe mapping: Mg/Ca in planktonic foraminifera. *Geochemistry, Geophysics, Geosystems*, *6*, Q12P06. https://doi.org/10.1029/2005GC000973

Sadekov, A. Y., Eggins, S. M., Klinkhammer, G. P., & Rosenthal, Y. (2010). Effects of seafloor and laboratory dissolution on the Mg/Ca composition of *Globigerinoides sacculifer* and *Orbulina universa* tests—A laser ablation ICPMS microanalysis perspective. *Earth and Planetary Science Letters*, *292*(3–4), 312–324. https://doi.org/10.1016/j.epsl.2010.01.039

Schiebel, R., & Hemleben, C. (2017). *Planktic foraminifers in the modern ocean* (pp. 358). Springer. https://doi.org/10.1007/978-3-662-50297-6

Schweitzer, P. N., & Lohmann, G. P. (1991). Ontogeny and habitat of modern menardiiform planktonic foraminifera. *Journal of Foraminiferal Research*, *21*(4), 332–346. https://doi.org/10.2113/gsjfr.21.4.332

Spero, H. J., Bijma, J., Lea, D. W., & Bemis, B. E. (1997). Effect of seawater carbonate concentration on foraminiferal carbon and oxygen isotopes. *Nature*, *390*(6659), 497–500. https://doi.org/10.1038/37333

Spero, H. J., Eggins, S. M., Russell, A. D., Vetter, L., Kilburn, M. R., & Hönisch, B. (2015). Timing and mechanism for intratest Mg/Ca variability in a living planktic foraminifer. *Earth and Planetary Science Letters*, *409*, 32–42. https://doi.org/10.1016/j.epsl.2014.10.030

Stangeew, E. (2001). Distribution and isotopic composition of living planktonic foraminifera *N. pachyderma* (sinistral) and *T.* quinqueloba in the High Latitude North Atlantic (Dissertation) (pp. 98).

Steinhardt, J., Cléroux, C., Ullgren, J., de Nooijer, L., Durgadoo, J. V., Brummer, G.-J., & Reichart, G.-J. (2014). Anti-cyclonic eddy imprint on calcite geochemistry of several planktonic foraminiferal species in the Mozambique Channel. *Marine Micropaleontology*, *113*, 20–33. https://doi.org/10.1016/j.marmicro.2014.09.001

Steinhardt, J., de Nooijer, L. L. J., Brummer, G.-J., & Reichart, G.-J. (2015). Profiling planktonic foraminiferal crust formation: Profiling planktic foraminiferal crust. *Geochemistry, Geophysics, Geosystems*, *16*, 2409–2430. https://doi.org/10.1002/2015GC005752

Takagi, H., Kimoto, K., Fujiki, T., Saito, H., Schmidt, C., Kucera, M., & Moriya, K. (2019). Characterizing photosymbiosis in modern planktonic foraminifera. *Biogeosciences*, *16*(17), 3377–3396. https://doi.org/10.5194/bg-16-3377-2019

Vergnaud Grazzini, C. (1976). Non-equilibrium isotopic compositions of shells of planktonic foraminifera in the Mediterranean Sea. *Palaeogeography, Palaeoclimatology, Palaeoecology*, *20*(4), 263–276. https://doi.org/10.1016/0031-0182(76)90007-9

Watkins, C. S., Schmidt, M. W., & Hertzberg, J. E. (2021). Calibrating *Trilobatus sacculifer* Na/Ca ratios from Atlantic core-tops as a proxy for sea surface salinity. *Paleoceanography and Paleoclimatology*, *36*, e2021PA004277. https://doi.org/10.1029/2021PA004277

Wit, J. C., de Nooijer, L. J., Wolthers, M., & Reichart, G. J. (2013). A novel salinity proxy based on Na incorporation into foraminiferal calcite. *Biogeosciences*, *10*(10), 6375–6387. https://doi.org/10.5194/bg-10-6375-2013

Wycech, J., Kelly, D. C., & Marcott, S. (2016). Effects of seafloor diagenesis on planktic foraminiferal radiocarbon ages. *Geology*, *44*(7), 551–554. https://doi.org/10.1130/G37864.1